

1 **Microbial dynamics in a High-Arctic glacier forefield: a combined field, laboratory, and**
2 **modelling approach.**

3 James A. Bradley ^{1,2}, Sandra Arndt ², Marie Šabacká ¹, Liane G. Benning ^{3,4}, Gary L. Barker ⁵, Joshua
4 J. Blacker ³, Marian L. Yallop ⁵, Katherine E. Wright ¹, Christopher M. Bellas ¹, Jonathan Telling ¹,
5 Martyn Tranter ¹, Alexandre M. Anesio ¹

6
7 ¹ Bristol Glaciology Centre, School of Geographical Sciences, University of Bristol, BS8 1SS, UK

8 ² BRIDGE, School of Geographical Sciences, University of Bristol, BS8 1SS, UK

9 ³ School of Earth and Environment, University of Leeds, LS2 9JT, UK

10 ⁴ GFZ, German Research Centre for Geosciences, 14473 Potsdam, Germany

11 ⁵ School of Biological Sciences, University of Bristol, BS8 1SS, UK

12

13 Corresponding author: James A. Bradley, email: j.bradley@bristol.ac.uk

14

15 **Abstract:** Modelling the development of soils in glacier forefields is necessary in order to assess how
16 microbial and geochemical processes interact and shape soil development in response to glacier
17 retreat. Furthermore, such models can help us predict microbial growth and the fate of Arctic soils in
18 an increasingly ice-free future. Here, for the first time, we combined field sampling with laboratory
19 analyses and numerical modelling to investigate microbial community dynamics in oligotrophic
20 proglacial soils in Svalbard. We measured low bacterial growth rates and growth efficiencies (relative
21 to estimates from Alpine glacier forefields), and high sensitivity to soil temperature (relative to
22 temperate soils). We used these laboratory measurements to inform parameter values in a new
23 numerical model and significantly refined predictions of microbial and biogeochemical dynamics of
24 soil development over a period of roughly 120 years. The model predicted the observed accumulation
25 of autotrophic and heterotrophic biomass. Genomic data indicated that initial microbial communities
26 were dominated by bacteria derived from the subglacial environment, whereas older soils hosted a
27 mixed community of autotrophic and heterotrophic bacteria. This finding was validated by the
28 numerical model, which showed that active microbial communities play key roles in fixing and
29 recycling carbon and nutrients. We also demonstrated the role of allochthonous carbon and microbial
30 necromass in sustaining a pool of organic material, despite high heterotrophic activity in older soils.
31 This combined field, laboratory and modelling approach demonstrates the value of integrated model-
32 data studies to understand and quantify the functioning of the microbial community in an emerging
33 High-Arctic soil ecosystem.

34

35 **Key words**

36 Glacier forefield

37 Microbial dynamics

38 Soil development

39 Numerical modelling

40 Integrated field-laboratory-modelling

41 SHIMMER

42

43 **1. Introduction**

44 Polar regions are particularly sensitive to anthropogenic climate change (Lee, 2014) and have
45 experienced accelerated warming in recent decades (Johannessen et al., 2004; Serreze et al., 2000;
46 Moritz et al., 2002). The response of terrestrial Polar ecosystems to this warming is complex. Warmer
47 conditions may increase soil respiration contributing to a positive feedback effect resulting from an
48 increase in CO₂ efflux to the atmosphere. This will lead to further warming induced by the greenhouse
49 effect (Billings, 1987; Oechel et al., 1993; Goulden et al., 1998). However, Arctic soils in particular
50 may over several decades acclimatize to warming due to an increase in primary productivity,
51 generating a net sink of CO₂ during the summer (Oechel et al., 2000). Accordingly, research to
52 understand the response of terrestrial ecosystems in high latitudes to environmental change is of
53 increasing importance. A visible consequence of Arctic warming is the large-scale retreat of glacier
54 and ice cover (ACIA, 2005; Paul et al., 2011; Staines et al., 2014; Dyurgerov and Meier, 2000). From
55 underneath the ice, a new terrestrial biosphere emerges, playing host to an ecosystem which may
56 exert an important influence on biogeochemical cycles, and more specifically atmospheric CO₂
57 concentrations and associated climate feedbacks (Dessert et al., 2003; Anderson et al., 2000;
58 Smittenberg et al., 2012; Berner et al., 1983). Furthermore, such a dramatic change will also
59 invariably affect global methane budgets (Kirschke et al., 2013), the phosphorus cycle (Filippelli,
60 2002; Follmi et al., 2009) and the productivity of downstream and coastal ecosystems (Anesio et al.,
61 2009; Mindl et al., 2007; Fountain et al., 2008; Anderson et al., 2000).

62

63 Numerous studies have attempted to characterize the physical and biological development of recently
64 exposed soils using a chronosequence approach, whereby a transect perpendicular to the retreating
65 ice snout represents a time sequence with older soils at increasing distance from the ice snout
66 (Schulz et al., 2013). We have recently shown that microbial biomass and macronutrients (such as
67 carbon, phosphorus and nitrogen) can accumulate in soils over timescales of decades to centuries
68 (Bradley et al., 2014). In such pristine glacial forefield soils the activity of microbial communities is
69 thought to be responsible for this initial accumulation of carbon and nutrients. Such an accumulation
70 facilitates colonization by higher order plants, leading to the accumulation of substantial amounts of
71 organic carbon (Insam and Haselwandter, 1989). However, organic carbon may also be derived from
72 allochthonous sources such as material deposited on the soil surface (from wind, hydrology,
73 precipitation and ornithogenic sources) and ancient organic pools derived from under the glacier
74 (Schulz et al., 2013). Nevertheless, the relative significance of allochthonous and autochthonous
75 sources of carbon to forefield soils, as well as their effect on ecosystem behavior are so far still poorly
76 understood (Bradley et al., 2014). Moreover, cycling of bioavailable nitrogen (which is derived from
77 active nitrogen-fixing organisms, allochthonous deposition, and degradation of organic substrates)
78 and phosphorus (liberated from the weathering of minerals and decomposition of organic substrates)
79 are similarly poorly quantified.

80

81 Several studies have observed shifts in the microbial community inhabiting pro-glacial soils of various
82 ages (Zumsteg et al., 2012; Zumsteg et al., 2011). This was expressed in increasing rates of
83 autotrophic and bacterial production with soil age (Schmidt et al., 2008; Zumsteg et al., 2013;
84 Esperschütz et al., 2011; Frey et al., 2013) and the overall decline in quality of organic substrates in
85 older soils (Goransson et al., 2011; Insam and Haselwandter, 1989). However, current evidence is
86 limited to mostly descriptive approaches, which may be challenging to interpret due to inherent
87 difficulties in disentangling interacting microbial and geochemical processes across various temporal
88 and spatial scales. Furthermore, the inherent heterogeneity of glacial forefield soils makes the
89 development of a single conceptual model that fits all challenging. Accordingly, pro-glacial
90 biogeochemical processes that dominate such systems remain poorly quantified and highly under-
91 explored. This current lack of understanding limits our ability to predict the future evolution of these
92 emerging landscapes and the potential consequences on global climate. Numerical models present
93 an opportunity to expand our knowledge of glacier forefield ecosystems by analytically testing the
94 hypotheses that arise from observations, extrapolating, interpolating and budgeting processes, rates
95 and other features to explore beyond the possibility of empirical observation (Bradley et al., 2016).
96 With such a model we can then also explore the sensitivity and resilience of these ecosystems to
97 environmental change.

98
99 Here, we have combined field observations, with laboratory incubations and elemental measurements
100 as well as genomic analyses and used these in a numerical model to investigate the development of
101 soils in a glacial forefield. With this data we refined some model parameters in the recently developed
102 **Soil biogeochemical Model for Microbial Ecosystem Response** (SHIMMER 1.0; Bradley et al. (2015))
103 model and applied this to the emerging forefield of the Midtre Lovénbreen glacier in Svalbard. The
104 Midtre Lovénbreen forefield is an ideal site to test the field-laboratory-model approach due to the lack
105 of vegetation during the first century of soil development, as this would obscure the microbial
106 community dynamics and considerably alter the physical properties of the soil (Brown and
107 Jumpponen, 2014; Ensign et al., 2006; King et al., 2008; Kastovska et al., 2005; Schutte et al., 2009;
108 Duc et al., 2009). The model development was informed by decades of empirical research on glacier
109 forefield soils, and has already been tested and validated using published datasets from the Damma
110 Glacier in Switzerland and the Athabasca Glacier in Canada. A thorough sensitivity analysis
111 highlighted the most important parameters to constrain in order to make further predictions more
112 robust. All our model parameter values are specific to individual, local model conditions and inherently
113 contain necessary model simplifications, abstractions and assumptions. Nevertheless, our earlier
114 sensitivity analyses revealed the following highly sensitive key parameters as the most important to
115 constrain through measurements: the maximum heterotrophic growth rate (I_{maxH}), the bacterial growth
116 efficiency (BGE, parameter Y_H) and the temperature response (Q_{10}).

117
118 Therefore, in this current study, we combined detailed field measurements with specifically designed
119 laboratory experiments and quantified values for these three parameters with a specific set of soils
120 from for the Midtre Lovénbreen forefield. The laboratory experiments and measurements were

121 conducted with the objective to better constrain these sensitive parameters. We then ran model
122 simulations in order to explore the ranges of model output and refine model predictions. Next, we
123 examined model output to explore the microbial and biogeochemical dynamics of recently exposed
124 soils in the Midtre Lovénbreen catchment and evaluate two main hypotheses. First, we tested the
125 hypothesis that microbial biomass in recently exposed soils accumulates due to *in situ* bacterial
126 growth and activity. It is commonly observed in glacier forefields that microbial biomass accumulates
127 with increasing soil age following exposure (Bernasconi et al., 2011; Schulz et al., 2013; Bradley et
128 al., 2014). This study provides a new quantitative and process-focused approach to examine *in situ*
129 growth in pioneer ecosystems, and assess the role of different functional groups in biomass
130 accumulation. Second, we tested the hypothesis that carbon fluxes in very recently exposed soils are
131 low, and are dominated by (abiotic) deposition of allochthonous substrate, whereas carbon fluxes are
132 high in older soils due to increased microbial (biotic) activity (such as microbial growth, respiration and
133 cell death). Increased soil carbon fluxes with soil age have been linked to microbial activity from the
134 forefield of the Damma Glacier, Switzerland (Smittenberg et al., 2012; Guelland et al., 2013b). With
135 this combined model, field and lab study, we were able to estimate carbon fluxes between ecosystem
136 components with daily resolution, and provide new insight into the interplay of processes that
137 contribute to net ecosystem production and soil organic carbon stocks in a High-Arctic system.

138

139 **2. Methods**

140 **2.1. Study site and sampling**

141 Midtre Lovénbreen is an Arctic polythermal valley glacier on the south side of Kongsfjorden, Western
142 Svalbard (latitude 78°55'N, longitude 12°10'E) (Fig. 1). The Midtre Lovénbreen catchment is roughly 5
143 km East of Ny-Ålesund, where several long-term monitoring programs have provided a wealth of
144 contextual information. Midtre Lovénbreen has experienced negative mass balance throughout much
145 of the 20th century. Since the end of the Little Ice Age (maximum in Svalbard in the 1900s) the de-
146 glaciated surface area of the Midtre Lovénbreen catchment has increased considerably in response to
147 warming mean annual temperatures. This continues to the present day. Between 1966 and 1990 ~
148 2.3 km² of land was exposed (Fleming et al., 1997; Moreau et al., 2008). We used a chronosequence
149 approach to determine ages for soils based on satellite imagery (Landsat TM 7) and previously
150 determined soil ages by aerial photography and carbon-14 dating techniques in Hodkinson et al.
151 (2003). Soil samples were collected along a transect perpendicular to the glacier snout, representing
152 soil ages of 0, 3, 5, 29, 50, and 113 years (Fig. 1) during the field season (18 July to 29 August 2013).
153 At each of the 6 sites along the chronosequence, 10 meter traverses roughly parallel to the glacier
154 snout were established and at each site 3 soil plots were sampled (using ethanol sterilized sampling
155 equipment). After removing the > 2 cm rock pieces at each site, about 100 grams of soil was collected
156 from the top 15 cm and immediately placed into sterile high-density polyethylene bags (Whirl-Pak
157 (Lactun, Australia)) that were frozen and stored at -20°C, and transported to the laboratories in the
158 Universities of Bristol and Leeds (UK).

159

160 **2.2. Laboratory analyses**

161 For bacterial abundance, samples were thawed and aliquots (100 mg) were immediately transferred
162 into sterile 1.5 mL micro-centrifuge (Eppendorf) tubes, where they were diluted with 900 μ L of Milli-Q
163 water (0.2 μ m filtered) and immediately fixed in 100 μ L glutaraldehyde (0.2 μ m filtered, 2.5% final
164 concentration). Samples were then vortexed for 10 seconds and sonicated for 1 minute at 30°C to
165 facilitate cell detachment from soil particles. Then 10 μ L fluorochrome DAPI (4', 6-diamidino-2
166 phenylindole) was added to half of the samples, tubes were vortexed briefly (3 seconds) and
167 incubated in the dark for 10 minutes, to be counted under UV light. The other half of each sample
168 remained untreated, for counting under auto-fluorescent light for photosynthetic pigmentation.
169 Samples were vortexed for 10 seconds and let stand for a further 30 seconds to ensure a well-mixed
170 solution, prior to filtering 100 μ L of the mixed liquid sample onto black Millipore Isopore membrane
171 filters (0.2 μ m pore size, 25 mm diameter), rinsed with a further 250 μ L of Milli-Q water (0.2 μ m
172 filtered). Bacterial cells were then counted using an Olympus BX41 microscope at 1000 times
173 magnification. The filtering apparatus was washed out with Milli-Q water between each filtration, and
174 negative control samples, prepared using Milli-Q water, were included into each series. A negative
175 control was a sample with no visible stained or auto-fluorescing cells. Thirty random grids (each 10⁴
176 μ m²) were counted per sample. Cell morphologies were measured and cell volume was estimated
177 and converted to carbon content according to Bratbak and Dundas (1984) (see Supplementary
178 Information). Separate aliquots of soil from each site were weighed after thawing and then dried at
179 105°C to obtain an estimate of soil moisture content.

180

181 Environmental DNA was isolated from at least 3 replicates for each soil age using MoBio PowerSoil®
182 DNA Isolation Kit and by following the instruction manual. The isolated 16S rDNA was amplified with
183 bacterial primers 515f (5'-GTGYCAGCMGCCGCGGTAA-3') and 926r (5'-
184 CCGYCAATTYMTTTRAGTTT-3'), creating a single amplicon of ~400 bp. The reaction was carried
185 out in 50 μ L volumes containing 0.3 mg mL⁻¹ Bovine Serum Albumin, 250 μ M dNTPs, 0.5 μ M of each
186 primer, 0.02 U Phusion High-Fidelity DNA Polymerase (Finnzymes OY, Espoo, Finland) and 5x
187 Phusion HF Buffer containing 1.5 mM MgCl₂. The following PCR conditions were used: initial
188 denaturation at 95°C for 5 minutes, followed by 25 cycles consisting of denaturation (95°C for 40
189 seconds), annealing (55°C for 2 minutes) and extension (72°C for 1 minute) and a final extension step
190 at 72°C for 7 minutes. Samples were sequenced using the Ion Torrent platform (using Ion 318v2 chip)
191 at Bristol Genomics facility at the University of Bristol. A non-barcoded library was prepared from the
192 amplicon pool using Life technologies Short Amplicon Prep Ion Plus Fragment Library Kit. The
193 template and sequencing kits used were: Ion PGM Template OT2 400 Kit and Ion PGM Sequencing
194 400 kit. The sequencing yielded 4.38 million reads. The 16S sequences were further processed using
195 MOTHUR (v. 1.35) and QIIME pipelines (Schloss et al., 2009; Caporaso et al., 2010). Chimeric
196 sequences were identified and removed using UCHIME (Edgar et al., 2011) and reads were clustered
197 into operational taxonomical units (OTUs), based on at least 97% sequence similarity, and assigned
198 taxonomical identification against Greengenes bacterial database (McDonald et al., 2012).

199

200 The carbon contents in the year 0 soils were analyzed with a Carlo-Erba elemental analyzer
201 (NC2500) at the German Research Center for Geosciences, Potsdam, Germany. The soils were oven
202 dried at 40°C for 48 hours, sieved to <7 mm and crushed using a TEMA disk mill to achieve size
203 fractions of < 20 µm. Total organic carbon (TOC) was analyzed after reacting the powders with a 10%
204 HCl solution for 12 hours to remove inorganic carbonates.

205

206 **2.3. Determination of maximum growth rates**

207 The microbial activity was determined in 113 year old soil samples after they were thawed (in the dark
208 at 5°C to mimic typical field temperature) for 168 hours. This age was chosen because these soil
209 samples were assumed to be the ones with the highest microbial biomass and activity and thus the
210 most appropriate for all laboratory measurements. In order to mitigate the effect of variability derived
211 from differences in soil properties between soil ages (that will later be predicted by the model),
212 laboratory experiments were conducted on a single soil age, with replicate incubations to assess the
213 possible variability in rates (and thus parameter values) that can be attributed to experimental
214 procedures and measurement techniques.

215

216 Aliquots of the soils were divided into petri dishes (25 g of soil (wet weight) into each petri dish) for
217 subsequent treatments. In order to alleviate nutrient limitations and measure maximum growth rates,
218 four different nutrient conditions were simulated: (1) no addition of nutrients, (2) low (0.03 mg C g⁻¹,
219 0.008 mg N g⁻¹, 0.02 mg P g⁻¹), (3) medium (0.8 mg C g⁻¹, 0.015 mg N g⁻¹, 0.1 mg P g⁻¹) and (4) high
220 additions (2.4 mg C g⁻¹, 0.024 mg N g⁻¹, 0.3 mg P g⁻¹). The ranges and concentrations were informed
221 by similar experiments in recently exposed proglacial soils at the Damma Glacier, Switzerland
222 (Goransson et al., 2011). Nutrients (C₆H₁₂O₆ for C, NH₄NO₃ for N and KH₂PO₄ for P) (Sigma, quality
223 ≥99.0%) were dissolved in 2 mL Milli-Q water (0.2 µm filtered), and mixed into the soils using an
224 ethanol-sterilized spatula. Samples were incubated at 25°C (in keeping with the design of SHIMMER
225 and for comparison with previous plausible range (Bradley et al., 2015; Frey et al., 2010)) in the dark
226 for a further 72 hours with the lids on. Throughout the whole incubation time, at 24 hour intervals,
227 additional 2 mL aliquots of Milli-Q water (0.2 µm filtered) were added to maintain approximate soil
228 moisture conditions in each sample.

229

230 In these samples bacterial production was estimated by the incorporation of ³H-leucine using the
231 microcentrifuge method detailed in Kirchman (2001). After the initial 72 hour incubation period
232 quadruplicate sample aliquots from the petri dish incubations and two trichloroacetic acid (TCA) killed
233 control samples were incubated for 3 hours at 25°C for every nutrient treatment. Approximately 50 mg
234 of soil was transferred to sterile micro-centrifuge tubes (2.0 mL, Fischer Scientific). Milli-Q (0.2 µm
235 pre-filtered) water and ³H-leucine was added to a final concentration of 100 nM (optimum leucine
236 concentration was pre-determined by a saturation experiment, Fig. S1, Supplementary Information).
237 The incubation was terminated by the addition of TCA to each tube. Tubes were then centrifuged at
238 15,000 g for 15 minutes, the supernatant was aspirated with a sterile pipette and removed, and 1 ml
239 ice-cold 5% TCA was added to each tube. Tubes were then centrifuged again at 15,000g for 5

240 minutes, before again aspirating and removing the supernatant. 1mL ice-cold 80% ethanol was added
241 and tubes were centrifuged at 15,000 g for 5 minutes, before the supernatant was aspirated and
242 removed again and tubes were left to air dry for 12 hours. Finally, 1 mL of scintillation cocktail was
243 added, samples were vortexed, and then counted by liquid scintillation (Perkin Elmer Liquid
244 Scintillation Analyzer, Tri-Carb 2810 TR). Radioisotope activity of TCA-killed control samples was
245 always less than 1.1% of the measured activity in live samples. There was a positive correlation
246 between the amount of sediment added to the tubes and background counts representing
247 disintegrations per minute (DPM). Counts were individually normalized by the amount of sediments
248 (corrected for dry weight) used in each sample to discount for background DPM. Leucine
249 incorporation rates were converted into bacterial carbon production following the methodology of
250 Simon and Azam (1989). Bacterial abundance was estimated from each treatment after the 72 hour
251 incubation period by microscopy. Five samples from each petri dish were counted for each nutrient
252 treatment with negative controls yielding no detectable cells. One-way ANOVA (with post-hoc Tukey
253 HSD) statistical tests were used for evaluations of the variability from the multiple treatments.

254

255 **2.4. Temperature response**

256 Microbial community respiration was determined by measuring CO₂ gas exchange rates in airtight
257 incubation vials. Soil samples from the 113 year old site were defrosted and divided (25 g wet weight)
258 in petri dishes as above, and 2 mL of Milli-Q water (0.2 µm filtered) was added (to maintain
259 consistency of soil moisture with determination of bacterial production above). Samples were
260 incubated at 5°C (T₁) and 25°C (T₂) in the dark for a further 72 hours. 2mL of 0.2 µm pre-filtered Milli-
261 Q water was added to the T₁ sample (3 mL for T₂) at 24, 48 and 72 hours to maintain approximate soil
262 moisture content. Two separate killed control tests (one furnaceed at 450°C for 4 hours, and one
263 autoclaved (3 cycles at 121°C)) were incubated at T₁ and T₂. Quintuple live and killed samples
264 (roughly 1 g) were transferred into cleaned 20 mL glass vials (rinsed in 2% Decon, submersed in 10%
265 HCl for 24 hours, rinsed 3 times with Milli-Q water and furnaceed at 450°C for 4 hours). These were
266 sealed (9°C, atmospheric pressure, ambient CO₂ of 405 ppm) with pre-sterilized Bellco butyl stoppers
267 (pre-sterilized by boiling for 4 hours in 1M sodium hydroxide) and crimped shut with aluminum caps.
268 Sealed vials were then incubated at T₁ and T₂ for 24 hours in darkness. After 24 hours, the
269 headspace gas was removed with a gas-tight syringe and immediately analyzed on an EGM4 gas
270 analyzer (PP Systems, calibrated using gas standards matching the expected range, precision 1.9%,
271 2*SE). Empty pre-sterilized vials were also incubated and analyzed. Following gas analysis, vials
272 were opened and dried to a constant weight at 105°C to estimate moisture content and thus dry soil
273 weight of these aliquots. Headspace CO₂ change (ppm) was converted to microbial respiration using
274 the ideal gas law ($n=PV/RT$), assuming negligible changes in soil pore water pH (and therefore CO₂
275 solubility) during the incubation. CO₂ headspace changes resulting from killed controls and blanks
276 were < 70% of the changes resulting from the incubations at T₁, and <7% of the changes observed at
277 T₂. One-way ANOVA (with post-hoc Tukey HSD) statistical tests were used for comparison of multiple
278 treatments. No significant differences in CO₂ headspace change between killed controls at T₁ and T₂
279 were detected (P=0.95).

280

281 **2.5. Microbial Model: SHIMMER**

282 SHIMMER (Bradley et al., 2015) mechanistically describes and predicts transformations in carbon,
283 nitrogen and phosphorus through aggregated components of the microbial community as a system of
284 interlinked ordinary differential equations. The model contains pools of microbial biomass, organic
285 matter and both dissolved inorganic and organic nitrogen and phosphorus (Table 1). It categorizes
286 microbes into autotrophs (A_{1-3}) and heterotrophs (H_{1-3}), and further subdivides these based on 3
287 specific functional traits. Microbes derived from underneath the glacier (referred to as “subglacial
288 microbes”) are termed A_1 and H_1 . A_1 are chemolithoautotrophic, obtaining energy from the oxidation
289 and reduction of inorganic compounds and carbon from the fixation of carbon dioxide. In contrast, H_1
290 rely on the breakdown of organic molecules for energy to support growth. A_2 and H_2 represent
291 autotrophic and heterotrophic microbes commonly found in glacier forefield soils with no “special”
292 characteristics, and will be referred to as “soil microbes”. A_3 and H_3 are autotrophs and heterotrophs
293 that are able to fix atmospheric N_2 gas as a source of nitrogen in cases when dissolved inorganic
294 nitrogen (DIN) stocks become limiting. Available organic substrate is assumed to be derived naturally
295 from dead organic matter and allochthonous inputs. Labile compounds are immediately available
296 fresh and highly reactive material, rapidly turned over by the microorganisms (S_1 , ON_1 , OP_1).
297 Refractory compounds are less bioavailable and represents the bulk of substrate present in the non-
298 living organic component of soil (S_2 , ON_2 , OP_2). A conceptual diagram showing the components and
299 transfers of SHIMMER is presented in the Supplementary Information (Fig. S2).

300

301 Microbial biomass responds dynamically to changing substrate and nutrient availability (expressed as
302 Monod-kinetics), as well as changing environmental conditions (such as temperature and light). A Q_{10}
303 temperature response function (T_i) is affixed to all metabolic processes including growth rates and
304 death rates (Bradley et al., 2015), thus effectively slowing down or speeding up all life processes as
305 temperature changes (Soetaert and Herman, 2009; Yoshitake et al., 2010; Schipper et al., 2014).
306 Light limitation is expressed as Monod kinetics. The following external forcings drive and regulate the
307 system’s dynamics:

- 308 • Photosynthetically-active radiation (PAR) (wavelength of approximately 400 to 700 nm) ($W\ m^{-2}$).
- 309
- 310 • Snow depth (m).
- 311 • Soil temperature ($^{\circ}C$).
- 312 • Allochthonous inputs ($\mu g\ g^{-1}\ day^{-1}$).

313

314 The model is 0-D and represents the soil as a homogeneous mix. Thus, light, temperature, nutrients,
315 organic compounds and microbial biomass are assumed to be evenly distributed.

316

317 Soil temperature (at 1 cm depth) for the entire of 2013 is provided by Alfred Wegener Institute for
318 Polar and Marine Research (AWI) from the permafrost observatory near Ny-Ålesund, Svalbard.

319 Similarly, PAR for 2013 are measured at the AWI surface radiation station near Ny-Ålesund,

320 Svalbard. Averaged daily snow depth for 2009 to 2013 is provided by the Norwegian Meteorological
321 Institute (eKlima). Allochthonous nutrient fluxes (inputs and leaching) are estimated based on an
322 evaluation of nutrient budgets of the Midtre Lovénbreen catchment (Hodson et al., 2005) in which
323 budgets for nutrient deposition rates and runoff concentrations are measured over two full summer-
324 winter seasons and residual retention rates (excess of inputs) or depletion rates (excess of outputs)
325 are inferred. The bioavailability of allochthonous material is assumed to be the same as initial material
326 and microbial necromass.

327

328 Initial conditions were informed by analysis of 0-years-of-exposure soil collected adjacent to the ice
329 snout, and initial values for all state variables are presented in Table 1. Initial microbial biomass was
330 estimated by microscopy as described above. Initial community structure was derived by 16S analysis
331 of year-0 soils. An initial value for carbon substrate ($S_1 + S_2$) was estimated based on the average
332 TOC content of year-0 soil. Bioavailability of model TOC was assumed to be 30% labile (S_1) and 70%
333 refractory (S_2) (for consistency with Bradley et al. (2015)). Organic nitrogen (ON) and organic
334 phosphorus (OP) were assumed to be stoichiometrically linked by the measured C:N:P ratio from the
335 Damma Glacier forefield (from which the model was initially developed and tested (Bradley et al.,
336 2015)). An initial value for DIN was taken from a previous evaluation of Svalbard tundra nitrogen
337 dynamics, whereby the lowest value is taken to represent the soil of least development, according to
338 traditional understanding of glacier forefields (Alves et al., 2013; Bradley et al., 2014). An initial value
339 for dissolved inorganic phosphorous (DIP) was established stoichiometrically from previous model
340 development and testing.

341

342 Model implementation and set-up is described in more detail in the Supplementary Information.

343

344 **2.6. Model parameters**

345 Maximum heterotrophic growth rate I_{maxH} (day^{-1}) was estimated by scaling the measured rate of
346 bacterial production ($\mu\text{g C g}^{-1} \text{day}^{-1}$) (converted to dry weight) with total heterotrophic biomass ($\mu\text{g C g}^{-1}$)
347 1). Nutrient addition alleviates growth limitations as defined in SHIMMER (Bradley, 2015); thus
348 bacterial communities can be assumed to be growing at I_{maxH} under experimental conditions.

349

350 Y_H represents heterotrophic BGE, and was estimated according to the equation:

351

$$352 \quad Y_H = \frac{BP}{BP + BR} \quad (1)$$

353 Where BP is and BR are measured bacterial production and measured bacterial respiration ($\mu\text{g C g}^{-1}$
354 day^{-1}) respectively, at 25°C with no nutrients added.

355

356 The temperature response (Q_{10}) value was estimated as:

357

358

359
$$Q_{10} = \left(\frac{R_2}{R_1} \right)^{\left(\frac{10}{T_2 - T_1} \right)}$$

360 (2)

361 Where R_1 and R_2 represent the measured respiration rate ($\mu\text{g C g}^{-1} \text{ day}^{-1}$) at temperatures T_1 and T_2
 362 (5°C and 25°C).

363
 364 Laboratory-defined parameters (i.e. growth rate, temperature sensitivity and BGE) were assumed to
 365 be the same for all microbial groups. A complete list of parameters and values is presented in Table
 366 S3 (Supplementary Information).

367

368 3. Results

369 3.1. Laboratory results and model parameters

370 Bacterial production in untreated soil was estimated at $0.76 \mu\text{g C g}^{-1} \text{ day}^{-1}$ ($\text{SD}=0.12$), and across all
 371 nutrient treatments ranged from 0.560 to $2.196 \mu\text{g C g}^{-1} \text{ day}^{-1}$. Nutrient addition led to increased
 372 measured production (low = $0.69 \mu\text{g C g}^{-1} \text{ day}^{-1}$ ($\text{SD}=0.12$), medium = $1.09 \mu\text{g C g}^{-1} \text{ day}^{-1}$ ($\text{SD}=0.53$),
 373 high = $1.52 \mu\text{g C g}^{-1} \text{ day}^{-1}$ ($\text{SD}=0.63$)), however variability between replicates was also high and
 374 production rates from each nutrient treatment were not significantly different from untreated soil
 375 ($P_{\text{low}}=0.99$, $P_{\text{medium}}=0.70$, $P_{\text{high}}=0.10$). The increased bacterial production was cross-correlated with
 376 quadruplicate measurements of biomass from each treatment, and resulting growth rates for all
 377 treatments were within a narrow range (0.359 to 0.550 day^{-1}) and there was no statistically significant
 378 difference in growth rates between each nutrient treatment (Fig. 2b) ($P_{\text{low-medium}}=0.55$, $P_{\text{medium-high}}=0.49$,
 379 $P_{\text{none-high}}=0.10$). The maximum measured growth rate for a single nutrient treatment, thus equating to
 380 the parameter I_{maxH} , was 0.55 day^{-1} . The 95% confidence range for I_{maxH} is 0.50 to 0.60 day^{-1} . This
 381 value is, to our knowledge, is the first measured rate of bacterial growth from High-Arctic soils, and
 382 falls within the lower end of the plausible range established in Bradley et al. (2015) ($0.24 - 4.80 \text{ day}^{-1}$)
 383 (Fig. 3a) for soil microbes from a range of laboratory and modelling studies (Frey et al., 2010;
 384 Ingwersen et al., 2008; Knapp et al., 1983; Zelenev et al., 2000; Stapleton et al., 2005; Darrah, 1991;
 385 Blagodatsky et al., 1998; Vandewerf and Verstraete, 1987; Foereid and Yearsley, 2004; Toal et al.,
 386 2000; Scott et al., 1995). For respiration, significantly higher CO_2 headspace concentration were
 387 detected in the live incubations at 25°C relative to killed controls ($P < 0.05$). Average respiration rate
 388 at 5°C was $1.61 \text{ C g}^{-1} \text{ day}^{-1}$ and there was a significant increase in soil respiration at 25°C ($12.83 \mu\text{g C}$
 389 $\text{g}^{-1} \text{ day}^{-1}$) (Fig. 2c) ($P < 0.05$). The Q_{10} value for Midtre Lovénbreen forefield soils was thus calculated
 390 as 2.90 , and a 95% confidence range was established as 2.65 to 3.16 . This was at the upper end of
 391 the plausible range previously identified in Bradley et al. (2015) (Fig. 3b). Based on measured values
 392 of bacterial production and respiration, BGE (Y_H) was 0.06 , with a 95% confidence range of 0.05 to
 393 0.07 (Fig. 3c). Final calculated values for model parameters are summarized in Table S3
 394 (Supplementary Information).

395

396 The results from microscopy determination of biomass are presented in Table 2. In the freshly
 397 exposed soil (year 0) heterotrophic biomass was low ($0.059 \mu\text{g C g}^{-1}$), increased substantially to 0.244

398 $\mu\text{g C g}^{-1}$ in 29 year old soils, and was an order or magnitude higher ($2.00 \mu\text{g C g}^{-1}$) in 113 year old
399 soils. Autotrophic biomass was considerably higher than heterotrophic biomass and increased by
400 roughly an order of magnitude from year 0 ($0.171 \mu\text{g C g}^{-1}$) to year 29 ($1.07 \mu\text{g C g}^{-1}$) and
401 approximately doubled by year 113 ($2.58 \mu\text{g C g}^{-1}$). TOC in freshly exposed soil was approximately
402 $0.793 \text{ mg C g}^{-1}$.

403

404 16S data was categorized into microbial groups (A_{1-3} and H_{1-3}) as defined by the model formulation.
405 Chemolithotrophs, such as known iron or sulfur oxidizers (genera *Acidithiobacillus*, *Thiobacillus*,
406 *Gallionella*, *Sulfurimonas*) were assigned into the A_1 group. Phototrophic microorganisms, such as
407 cyanobacteria (*Phormidium*, *Leptolyngbya*) and phototrophic bacteria (*Rhodospirillum rubrum*, *Erythrobacter*,
408 *Halomicronema*) were allocated into group A_2 , while heterocyst forming cyanobacteria from the orders
409 Nostocales and Stigonematales were assigned to group the A_3 (nitrogen-fixing autotrophs).
410 Members of the family Comamonadaceae of the Betaproteobacteria are known subglacial dwelling
411 microorganisms (Yde et al., 2010) and were thus included into the group H_1 . General soil
412 heterotrophic microorganisms (mainly members of Alphaproteobacteria, Actinobacteria,
413 Bacteroidetes and Acidobacteria) were assigned into group H_2 (general soil heterotrophs). Lastly,
414 group H_3 consisted of heterotrophic nitrogen fixers, mainly *Azospirillum*, *Bradyrhizobium*, *Devosia*,
415 *Clostridium*, *Frankia* and *Rhizobium*. Pathogens, non-soil microorganisms and organisms with
416 unknown physiological traits were assigned into "Uncategorized" group. Subglacial microbes
417 accounted for 43 to 45 % of reads in year 0 and 5, and declined in older soils (year 50 and 113) to 18
418 to 22%. The subglacial community was predominantly chemolithoautotrophic (A_1). Typical soil
419 bacteria (A_2 and H_2) increased from low abundance (30% and 40% in years 0 and 5 respectively) to
420 relatively high abundance (63 to 67%) of reads in years 50 and 113. Nitrogen fixing bacteria were
421 prevalent in recently exposed soils (14% in year 0) but low in relative abundance in soils above 5
422 years of age (4 to 6% in years 5, 50 and 113). In the freshly exposed soil (year 0), the microbial
423 community was relatively evenly distributed between heterotrophs (43%) and autotrophs (44%). In
424 developed soils, the relative abundance of heterotrophs increased (up to 74% of reads in years 50
425 and 113). Important to note is the fact that between 8 and 21% of the reads across all samples could
426 not be classified.

427

428 **3.2. Model Results**

429 The model predicted an accumulation of autotrophic and heterotrophic biomass over 120 years (Fig.
430 4a and 4b). Biomass and nutrient concentrations were initially extremely low (total biomass $< 0.25 \mu\text{g}$
431 C g^{-1} , DIN $< 4.0 \mu\text{g N g}^{-1}$, DIP $< 3.0 \mu\text{g P g}^{-1}$), and biological activity in initial soils was also low (Table
432 3). There was an order of magnitude increase in total microbial biomass in years 10 to 60. Nitrogen-
433 fixing autotrophs (A_3) and heterotrophs (H_3), and soil heterotrophs (H_2) experienced rapid growth
434 during this period. Subglacial and soil autotrophs (A_{1-2}) and subglacial heterotrophs (H_1) remained
435 low. Bacterial production increased by roughly two orders of magnitude (Table 3). Organic carbon
436 (labile and refractory) increased (Fig. 4c), whilst DIN and DIP concentrations increased by
437 approximately an order of magnitude in the first 60 years (Fig. 4d). During the later stages of soil

438 development (years 60 to 120), biomass increased rapidly due to the rapid growth of soil organisms
439 (A_2 and H_2), which outcompeted nitrogen-fixers. The model showed a rapid exhaustion of labile
440 organic carbon (years 50 to 100), while refractory carbon accumulated slowly. Nutrients (DIN and
441 DIP) accumulated at a relatively constant rate. Microbial activity, including bacterial production,
442 nitrogen fixation and DIN assimilation, was high relative to early stages (Table 3).

443

444 A carbon budget of fluxes through the substrate pool is presented in Fig. 5. Daily fluxes are presented
445 in panels (a) for year 5, (b) for year 50 and (c) for year 113, and annual fluxes up to year 120 are
446 presented in (d). In recently exposed soils (5 years), allochthonous inputs were the only noticeable
447 carbon flux, outweighing heterotrophic growth and respiration, and the contribution of substrate from
448 necromass and exudates by over two orders of magnitude (Fig. 5a). Thus, the total change in carbon
449 (black line) closely resembled allochthonous input. In the intermediate stages (Fig. 5b), there was
450 substantial depletion from the substrate pool due to heterotrophic activity. Heterotrophic growth (red
451 line) was low despite high substrate consumption and respiration (orange line). In the late stages of
452 soil development, the flux of microbial necromass was a significant contributor to the organic
453 substrate pools (Fig. 5c). Carbon fluxes in mid to late stages of soil development were highly
454 seasonal (Fig. 5b and 5c). Biotic fluxes (e.g. respiration) were up to six times higher during the
455 summer (July to September) compared to the winter (November to April), however a base rate of
456 heterotrophic respiration and turnover of microbial biomass was sustained over winter. Figure 4d
457 shows that the contribution of microbial necromass rose steadily throughout the simulation (blue line),
458 however was not sufficient to compensate the uptake of carbon substrate, thus leading to overall
459 depletion between years 50 to 110 (black line). The contribution of exudates (green line) to substrate
460 was minimal at all soil ages.

461

462 **4. Discussion**

463 **4.1. Determination of parameters and model predictions**

464 Figure 6 illustrates the influence of the site-specific, laboratory-derived parameters on microbial
465 biomass predictions. It compares the range of predicted microbial biomass based on laboratory-
466 determined parameters (yellow) to the entire plausible parameter range (red; Bradley et al. (2015)).
467 Predicted biomass with the average laboratory-derived value is indicated by the black line. For I_{max} ,
468 predicted biomass with laboratory-derived parameters (yellow shading) was towards the lower end of
469 the plausible range (Fig. 6a) because refined growth rates were significantly lower than the maximum
470 values explored previously. This was mostly due to a significant reduction in autotrophic biomass (A_1 -
471 $_3$). With high growth rates, there was a sharp early increase in biomass (years 10 to 20) followed by
472 slower growth phase (years 20 to 120). Model results with laboratory-derived growth rates showed
473 that the exponential growth phase occurred later (years 40 to 80) and was more prolonged, but total
474 biomass was considerably lower. There was a substantial reduction in the plausible range in predicted
475 microbial biomass.

476

477 There was a substantial reduction in the plausible range in predicted microbial biomass (Fig. 6b) from
478 the measured temperature sensitivity (Q_{10}) (yellow) compared to the previous range (red). Soil
479 microbial communities in Polar regions must contend with extremely harsh environmental conditions
480 such as cold temperatures, frequent freeze-thaw cycles, low water availability, low nutrient availability,
481 high exposure to ultraviolet radiation in the summer, and prolonged periods of darkness in winter.
482 These factors profoundly impact their metabolism and survival strategies and ultimately shape the
483 structure of the microbial community (Cary et al., 2010). High Q_{10} values, as derived here, are typical
484 of cold environments and cold adapted organisms and this has been associated with the survival of
485 biomass under prolonged periods of harsh environmental conditions (Schipper et al., 2014). An
486 investigation into the metabolism of microbial communities in biological soils crusts in recently
487 exposed soils from the East Brøgger Glacier, approximately 6 km from the Midtre Lovénbreen
488 catchment, also derived a high Q_{10} (3.1) (Yoshitake et al., 2010). The Midtre Lovénbreen catchment,
489 in Svalbard, experiences a relatively extreme Arctic climate. The high Q_{10} ultimately lowers the overall
490 rate of biomass accumulation in ultra-oligotrophic soils and a baseline population is maintained.

491

492 The low measured BGE (0.06) suggested that a high proportion (94%) of substrate consumed by
493 heterotrophs is remineralized (degrading organic substrate into DIC (CO_2), DIN and DIP), with very
494 little being incorporated into biomass (6%). Low BGE encouraged the liberation and release of
495 nutrients to the soil and thus the overall growth response of the total microbial biomass was more
496 rapid due to higher soil nutrient concentrations (Fig. 6c). However, due to the low BGE, there was a
497 high rate of substrate degradation, and as such, labile substrate was rapidly depleted when
498 heterotrophic biomass was high (Fig. 4c). Heterotrophic growth requires that a substantial amount of
499 substrate is degraded – thus, although autotrophic production outweighed heterotrophic production at
500 all stages of development (Fig. 4e), the soil was predicted by the model to be a net source of CO_2 to
501 the atmosphere over the first 120 years of exposure (Fig. 4f). There are very few measurements of
502 BGE in cold glaciated environments, however previous studies have suggested values as low as
503 0.0035 to 0.033 (Anesio et al., 2010; Hodson et al., 2007).

504

505 A major assumption of SHIMMER is that parameter values remain constant throughout the duration of
506 the simulation. Empirical evidence suggests that parameters defined as fixed in SHIMMER (e.g. Q_{10})
507 may be variable over time, however in SHIMMER, like many numerical modelling formulations,
508 changing environmental (temperature, light) and geochemical (carbon substrate, available nitrogen,
509 available phosphorus) conditions drive subsequent variability in microbial activity via mathematical
510 formulations (e.g. Monod kinetics, see Bradley et al. (2015)) affixed to parameter values. A second
511 major assumption is the assignment of measured rates to parameters for all microbial functional
512 groups. Rather than taxonomic based classification, SHIMMER distinguishes and classifies microbial
513 communities based on functional traits. These mathematical formulations assigned to, for example,
514 microbial growth, are different between groups to represent distinct functional traits associated with
515 that group. Whilst actual rates may be different between different organisms, for the level of model
516 complexity and outputs required, a community measurement of those parameters is sufficient,

517 particularly considering that the differences are accounted for in the mathematical formulation of
518 SHIMMER (see Bradley et al. (2015)).

519

520 **4.2. Microbial biomass dynamics and community structure**

521 Measured microbial biomass in the initial soils of Midtre Lovénbreen ($0.23 \mu\text{g C g}^{-1}$, 0 years) was very
522 low compared to initial soils in other deglaciated forefields of equivalent ages in lower latitudes, for
523 example in the Alps ($4 \mu\text{g C g}^{-1}$) (Bernasconi et al., 2011; Tscherko et al., 2003) and Canada ($6 \mu\text{g C}$
524 g^{-1}) (Insam and Haselwandter, 1989). However, our microbial biomass values are more similar to
525 other recently deglaciated soils in Antarctica (Ecology Glacier - $0.88 \mu\text{g C g}^{-1}$) (Zdanowski et al.,
526 2013). Low biomass is possibly a result of the harsh, ultra-oligotrophic and nutrient limiting
527 environment of the High Arctic and Antarctica, where low temperature and longer winters limit the
528 summer growth phase, especially compared to an Alpine system (Tscherko et al., 2003; Bernasconi
529 et al., 2011).

530

531 The initial microbial community structure in our samples was predominantly autotrophic (74.5%). In
532 the years following exposure, we observed an increase in autotrophs and heterotrophs with soil age
533 (Table 2), presumably due to the establishment and growth of stable soil microbial communities
534 (Schulz et al., 2013; Bradley et al., 2014). Both the observations and modelling results suggested that
535 there was no substantial increase in heterotrophic biomass during the initial and early-intermediate
536 stages of soil development (years 0 to 40), which was then followed by a growth phase whereby
537 biomass increased by roughly an order of magnitude. Overall, the model and the microscopy data
538 were in good agreement accounting for the limitations in both techniques, spatial heterogeneity, and
539 the oscillations in biomass arising from seasonality (Fig. 7). SHIMMER predicted that low initial
540 microbial populations have the potential to considerably increase in population density during several
541 decades of soil development. This data thus supports the hypothesis that the observed increase in
542 microbial biomass with soil age is a consequence of *in situ* growth and activity. The pattern of
543 microbial abundance observed in the Midtre Lovénbreen forefield broadly resembles that of other
544 glacier forefields worldwide (see Bradley et al. (2014)). For example, data from the Rootmoos Ferner
545 (Austria) (Insam and Haselwandter, 1989), Athabasca (Canada) (Insam and Haselwandter, 1989),
546 Damma (Switzerland) (Bernasconi et al., 2011; Schulz et al., 2013) and Puca (Peru) (Schmidt et al.,
547 2008) glacier forefields find increased microbial biomass and activity over decades to centuries of soil
548 development following exposure.

549

550 The genomic data indicated that subglacial microbes are dominant in recently exposed soils, in
551 agreement with model results (Fig. 8). The community structure in year 5 was heavily dominated by
552 chemolithoautotrophs (A_1), which reflected findings from previous studies whereby
553 chemolithoautotrophic bacteria contribute to the oxidation of FeS_2 in proglacial moraines in Midtre
554 Lovénbreen (Borin et al., 2010; Mapelli et al., 2011). These processes are also commonly described
555 in other subglacial habitats (Boyd et al., 2014; Hamilton et al., 2013). Based on 16S data, the
556 subglacial community declined in relative abundance with soil age. This finding was also reflected in

557 the model in years 50 and 113. As the age of the soil progressed, there was typically greater
558 abundance of microbes representing typical soil bacteria (groups A₂ and H₂) in the 16S data and the
559 model, thus the relative abundance of subglacial microbes decreased.

560

561 Microscopic analyses indicated low total biomass in recently exposed soils (up to 1.7 µg C g⁻¹ in soil
562 exposed for 50 years) that was comprised predominantly of autotrophic bacteria. Model simulations
563 agreed well with microscopy derived data. Overall, the 16S data, when categorised into functional
564 groups as defined by the model, agreed well with the microscopy and model output in the very early
565 stages of soil development. However, in later stages of soil development (50 years and older),
566 microscopy and modelling suggested a continuation of predominantly autotrophic soil microbial
567 communities whereas 16S sequence data notably indicated a predominantly heterotrophic
568 community. With extremely low biomass, cell counts derived from microscopy, as well as
569 representation of relative abundance by 16S extraction and amplification, can be largely skewed by
570 relatively small changes in the soil microbial community. Furthermore, the comparative difficulty to
571 lyse autotrophic bacteria (such as some groups of cyanobacteria) from an environmental sample
572 compared to heterotrophic bacteria, and thus successfully amplify the 16S gene during the PCR
573 process, may skew 16S sequence data in favour of heterotrophic sequence reads. Additionally,
574 SHIMMER is an ambitious model in that it attempts to simulate, predict and constrain multiple
575 functional types of bacteria species in a numerical framework. Numerical models containing multiple
576 species or multiple microbial functional groups are often extremely challenging to constrain (Servedio
577 et al., 2014; Hellweger and Bucci, 2009; Jessup et al., 2004; Larsen et al., 2012), and as such, the
578 majority of microbial soil models often only resolve one or two living biomass pool that represents the
579 bulk activity and function of the entire community (see e.g. Manzoni et al. (2004), Manzoni and
580 Porporato (2007), Blagodatsky and Richter (1998), Ingwersen et al. (2008), Wang et al. (2014) and
581 others). Our rationale for resolving six distinct functional groups was to quantitatively assess, using
582 modelling, the relative importance and role of each functional group at different stages of soil
583 development. Regardless of discrepancies in older soils (over 50 years since exposure), both the 16S
584 and microscopy data indicated that there was a mixed community of autotrophs and heterotrophs in
585 soils of all ages, which was supported by modelling, since no functional groups were extirpated over
586 simulations representing 120 years of soil development. Thus, SHIMMER is able to capture the
587 diversity of the samples over 120 years of soil development, but the detailed community composition
588 requires further investigation.

589

590 Nitrogen-fixing bacteria were prevalent in recently exposed soils but declined in relative abundance
591 with soil age. By fixing N₂ instead of assimilating DIN, the model predicted that nitrogen-fixers were
592 able to grow rapidly in the early stages relative to other organisms (Fig. 4a, 4b). The model prediction
593 supports findings by previous studies demonstrating the importance of nitrogen fixation in Alpine (Duc
594 et al., 2009; Schmidt et al., 2008) and Antarctic (Strauss et al., 2012) glacier forefields and other High-
595 Arctic (Svalbard, Greenland) glacial ecosystems (Telling et al., 2011; Telling et al., 2012). However,
596 there was poor agreement on the relative abundance of nitrogen-fixers between the model and the

597 16S data in the later stages of soil development (years 50 to 120), particularly between autotrophs
598 and heterotrophs. The model over-predicted the relative abundance of nitrogen-fixing organisms (Fig.
599 8). The majority of the biomass of the autotrophic nitrogen-fixers was composed of sequences
600 belonging to the cyanobacterium from the genus *Nostoc*. *Nostoc* forms macroscopically visible
601 colonies that grow on the surface of the soils. Its distribution in the Arctic soils is thus extremely
602 patchy and therefore, part of the discrepancy between the 16S data and the model regarding the
603 relative distribution of the A₃ group in the older soils could be due to under-sampling of the *Nostoc*
604 colonies as a consequence of a random sampling approach. Furthermore, allochthonous inputs of
605 nitrogen to the Arctic (e.g. aerial deposition (Geng et al., 2014)) strongly affect the productivity of
606 microbial ecosystems and the requirement of nitrogen fixation for microbes (Bjorkman et al., 2013;
607 Kuhnelt et al., 2013; Kuhnelt et al., 2011; Hodson et al., 2010; Telling et al., 2012; Galloway et al.,
608 2008). Thus, uncertainty in the allochthonous availability of nitrogen strongly affects nitrogen fixation
609 rates. In attempting to replicate a qualitative understanding of the nitrogen cycle in a quantitative
610 mathematical modelling framework, the predicted importance of nitrogen-fixing organisms may be
611 over-estimated. The poor agreement in the relative abundance of nitrogen-fixers between the model
612 and the 16S data indicates an incomplete understanding of allochthonous versus autochthonous
613 nutrient availability. Allochthonous nutrient availability is a known source of uncertainty (Bradley et al.,
614 2014; Schulz et al., 2013; Schmidt et al., 2008), and addressing this concern is the subject of future
615 work.

616

617 16S data is an exciting resource of information that is rarely (or never) used to test models. However,
618 the environment (difficulty to extract DNA), the presentation (percentages of low concentration and
619 thus easy to shift relative abundance) and model uncertainties make comparisons challenging. In
620 making this first attempt at comparison of model output to 16S data, we hope to spark discussion and
621 further development of approaches that have similar objectives in order to improve future model
622 performance.

623

624 **4.3. Net ecosystem metabolism and carbon budget**

625

626 Allochthonous carbon inputs were the most significant contributor to recently exposed soils (e.g. year
627 5), since the total change in substrate closely followed this flux (Fig. 5). In older soils (year 113), biotic
628 fluxes were substantially higher, and microbial necromass contributed equally as a source of organic
629 substrate compared to allochthonous deposition. In the older soils, heterotrophic growth and
630 respiration caused substantial consumption and thus depletion of available carbon stocks. This
631 evidence thus supports the hypothesis that carbon fluxes in very recently exposed soils are low and
632 are dominated by abiotic processes (i.e. allochthonous deposition), whereas biotic processes (such
633 as microbial growth, respiration and cell death) play a greater role in developed soils with increased
634 microbial abundance and activity. These findings for the Midtre Lovénbreen glacier in the High-Arctic,
635 are similar to what has been observed based on empirical evidence from Alpine settings (at the
636 Damma Glacier, Switzerland (Smittenberg et al., 2012; Guelland et al., 2013)).

637

638 The seasonality of carbon fluxes predicted by the model (Fig. 5b and 5c) related to the high measured
639 Q_{10} values. High seasonal variation in biotic fluxes and rates is typical of cryospheric soil ecosystems
640 (Schostag et al., 2015) including Alpine glacier forefield soils (Lazzaro et al., 2012; Lazzaro et al.,
641 2015). However, microbial activity has been shown to persist during winter under insulating layers of
642 snow and in sub-zero temperatures (Zhang et al., 2014). Modelling also predicted sustained organic
643 substrate degradation, microbial turnover and net heterotrophy during the winter (Fig. 5b and 5c), as
644 documented in other glacier forefield studies from an Alpine setting (Guelland et al., 2013b).

645

646 The low measured BGE has three important consequences. Firstly, low BGE suggests that a large
647 pool of substrate is required to support heterotrophic growth. Low-efficiency heterotrophic growth lead
648 to the rapid depletion of substrate; therefore high allochthonous inputs were required to maintain a
649 sizeable pool. In older soils (years 80 to 120), increased inputs from microbial necromass (blue line,
650 Fig. 5d) sustained substrate supply to heterotrophs. The sources of allochthonous carbon substrate to
651 the glacier forefield include meltwater inputs derived from the supraglacial and subglacial ecosystems
652 (Stibal et al., 2008; Hodson et al., 2005; Mindl et al., 2007), snow algae (which are known to be
653 prolific primary colonizers and producers in High Arctic snow packs (Lutz et al., 2015; Lutz et al.,
654 2014), atmospheric deposition (Kuhnel et al., 2013) and ornithogenic deposition (e.g. fecal matter of
655 birds and animals) (Jakubas et al., 2008; Ziolk and Melke, 2014; Luoto et al., 2015; Michelutti et al.,
656 2009; Michelutti et al., 2011; Moe et al., 2009). Microbial dynamics are moderately sensitive to
657 external allochthonous inputs of substrate (Bradley et al., 2015), and addressing the uncertainty
658 associated with this flux is an important question to address in future research.

659

660 Secondly, low BGE causes a net efflux of CO_2 over the first 120 years of soil development despite
661 high autotrophic production (Fig. 4e and 4f). Recent literature has explored the carbon dynamics of
662 glacier forefield ecosystems, finding highly variable soil respiration rates (Bekku et al., 2004; Schulz et
663 al., 2013; Guelland et al., 2013a). Future studies should focus on quantifying carbon and nutrient
664 transformations and the potential for forefield systems to impact global biogeochemical cycles in
665 response to future climate change (Smittenberg et al., 2012) and in the context of large-scale ice
666 retreat.

667

668 Thirdly, high rates of substrate degradation encouraged by low BGE were responsible for rapid
669 nutrient release. Modelling suggested that microbial growth was strongly inhibited by low nutrient
670 availability in initial soils ($4 \mu\text{g N g}^{-1}$, 2 to $10 \mu\text{g P g}^{-1}$) (Fig. 4d). This is consistent with findings from
671 the Hailuogou Glacier (Gongga Shan, China) and Damma Glacier (Switzerland) (Prietz et al., 2013).
672 Low BGE is predicted by the model to have a very important role in encouraging the release of
673 nutrients from organic material more rapidly, thereby increasing total bacterial production in the
674 intermediate stages of soil development. Increased nutrient availability with increased heterotrophic
675 biomass is consistent with recent observations from glacier forefields (Bekku et al., 2004; Schulz et
676 al., 2013; Schmidt et al., 2008).

677

678 **5. Conclusions**

679 We used laboratory-based mesocosm experiments to measure three key model parameters:
680 maximum microbial growth rate (I_{max}) (by incorporation of ^3H -leucine), BGE (Y) (by measuring
681 respiration rates) and the temperature response (Q_{10}) (by measuring rates at different ambient
682 temperatures). Laboratory-derived parameters were comparable with previous estimations. We
683 refined model predictions by narrowing the range of model output over nominal environmental
684 conditions, thus increasing confidence in model predictions. Our results demonstrated that *in situ*
685 microbial growth lead to the overall accumulation of microbial biomass in the Midtre Lovénbreen
686 forefield during the first century of soil development following exposure. Furthermore, carbon fluxes
687 increased in older soils due to elevated biotic (microbial) activity. Microbial dynamics at the initial
688 stages of soil development in glacial forefields do not contribute to significant accumulation of organic
689 carbon due to the very low growth efficiency of the microbial community, resulting in a net efflux of
690 CO_2 from those habitats. However, the low bacterial growth efficiency in glacial forefields is also
691 responsible for high rates of nutrient remineralization that most probably has an important role on the
692 establishment of plants at older ages. The relative importance of allochthonous versus autochthonous
693 substrate and nutrients is the focus of future research.

694

695 Much of the extreme ice-free regions in Antarctica are characterized by a complete absence of higher
696 order plants. However even these environments contain diverse microbial populations and extremely
697 low but detectable levels of organic carbon (Cowan et al., 2014), making these environments suitable
698 cases for modelling using SHIMMER. This exercise shows how an integrated model-data approach
699 can improve understanding and predictions of microbial dynamics in forefield soils and disentangle
700 complex process interactions to ascertain the relative importance of each process independently. This
701 would, for annual budgets, be extremely challenging with a purely empirical approach. Nevertheless,
702 more clarity and data are needed in tracing the dynamics and interactions of these carbon pools to
703 improve confidence and validate model simulations. This combined approach explored detailed
704 microbial and biogeochemical dynamics of soil development with the view to obtaining a more holistic
705 picture of soil development in a warmer and increasingly ice-free future world.

706

707 **Acknowledgements**

708 We thank Siegrid Debatin, Marion Maturilli, and Julia Boike (AWI) for support in acquiring
709 meteorological and radiation data, Simon Cobb and James Williams (University of Bristol) for
710 laboratory assistance, and Nicholas Cox and James Wake for assistance in the field and use of the
711 UK Station Arctic Research base in Ny-Ålesund. We also thank the two anonymous referees who
712 provided valuable comments on the manuscript. This research was supported by NERC grant no.
713 NE/J02399X/1 to A. M. Anesio. S. Arndt acknowledges support from NERC grant no. NE/IO21322/1.

714

715

716 **References**

717 ACIA: Arctic Climate Impacts Assessment, Cambridge University Press, Cambridge, 1042,
718 2005.

719 Alves, R. J. E., Wanek, W., Zappe, A., Richter, A., Svenning, M. M., Schleper, C., and Urich, T.:
720 Nitrification rates in Arctic soils are associated with functionally distinct populations of
721 ammonia-oxidizing archaea, *Isme J*, 7, 1620-1631, 10.1038/ismej.2013.35, 2013.

722 Anderson, S. P., Drever, J. I., Frost, C. D., and Holden, P.: Chemical weathering in the
723 foreland of a retreating glacier, *Geochim Cosmochim Acta*, 64, 1173-1189, Doi 10.1016/S0016-
724 7037(99)00358-0, 2000.

725 Anesio, A. M., Hodson, A. J., Fritz, A., Psenner, R., and Sattler, B.: High microbial activity on
726 glaciers: importance to the global carbon cycle, *Global Change Biol*, 15, 955-960, DOI
727 10.1111/j.1365-2486.2008.01758.x, 2009.

728 Anesio, A. M., Sattler, B., Foreman, C., Telling, J., Hodson, A., Tranter, M., and Psenner, R.:
729 Carbon fluxes through bacterial communities on glacier surfaces, *Ann Glaciol*, 51, 32-40,
730 2010.

731 Bekku, Y. S., Nakatsubo, T., Kume, A., and Koizumi, H.: Soil microbial biomass, respiration
732 rate, and temperature dependence on a successional glacier foreland in Ny-Alesund,
733 Svalbard, *Arct Antarct Alp Res*, 36, 395-399, 2004.

734 Bernasconi, S. M., Bauder, A., Bourdon, B., Brunner, I., Bunemann, E., Christl, I., Derungs, N.,
735 Edwards, P., Farinotti, D., Frey, B., Frossard, E., Furrer, G., Gierga, M., Goransson, H.,
736 Gulland, K., Hagedorn, F., Hajdas, I., Hindshaw, R., Ivy-Ochs, S., Jansa, J., Jonas, T., Kiczka, M.,
737 Kretzschmar, R., Lemarchand, E., Luster, J., Magnusson, J., Mitchell, E. A. D., Venterink, H.
738 O., Plotze, M., Reynolds, B., Smittenberg, R. H., Stahli, M., Tamburini, F., Tipper, E. T.,
739 Wacker, L., Welc, M., Wiederhold, J. G., Zeyer, J., Zimmermann, S., and Zumsteg, A.:
740 Chemical and Biological Gradients along the Damma Glacier Soil Chronosequence,
741 Switzerland, *Vadose Zone J*, 10, 867-883, Doi 10.2136/Vzj2010.0129, 2011.

742 Berner, R. A., Lasaga, A. C., and Garrels, R. M.: The Carbonate-Silicate Geochemical Cycle
743 and Its Effect on Atmospheric Carbon-Dioxide over the Past 100 Million Years, *Am J Sci*, 283,
744 641-683, 1983.

745 Billings, W. D.: Carbon Balance of Alaskan Tundra and Taiga Ecosystems - Past, Present and
746 Future, *Quaternary Sci Rev*, 6, 165-177, Doi 10.1016/S0277-3791(00)90007-6, 1987.

747 Bjorkman, M. P., Kuhnel, R., Partridge, D. G., Roberts, T. J., Aas, W., Mazzola, M., Viola, A.,
748 Hodson, A., Strom, J., and Isaksson, E.: Nitrate dry deposition in Svalbard, *Tellus B*, 65, Artn
749 19071
750 Doi 10.3402/Tellusb.V65i0.19071, 2013.

751 Blagodatsky, S. A., and Richter, O.: Microbial growth in soil and nitrogen turnover: A
752 theoretical model considering the activity state of microorganisms, *Soil Biol Biochem*, 30,
753 1743-1755, Doi 10.1016/S0038-0717(98)00028-5, 1998.

754 Blagodatsky, S. A., Yevdokimov, I. V., Larionova, A. A., and Richter, J.: Microbial growth in
755 soil and nitrogen turnover: Model calibration with laboratory data, *Soil Biol Biochem*, 30,
756 1757-1764, Doi 10.1016/S0038-0717(98)00029-7, 1998.

757 Borin, S., Ventura, S., Tambone, F., Mapelli, F., Schubotz, F., Brusetti, L., Scaglia, B., D'Acqui,
758 L. P., Solheim, B., Turicchia, S., Marasco, R., Hinrichs, K. U., Baldi, F., Adani, F., and
759 Daffonchio, D.: Rock weathering creates oases of life in a High Arctic desert, *Environ*
760 *Microbiol*, 12, 293-303, DOI 10.1111/j.1462-2920.2009.02059.x, 2010.

761 Boyd, E. S., Hamilton, T. L., Havig, J. R., Skidmore, M. L., and Shock, E. L.: Chemolithotrophic
762 Primary Production in a Subglacial Ecosystem, *Appl Environ Microb*, 80, 6146-6153,
763 10.1128/Aem.01956-14, 2014.

764 Bradley, J. A., Singarayer, J. S., and Anesio, A. M.: Microbial community dynamics in the
765 forefield of glaciers, *Proceedings. Biological sciences / The Royal Society*, 281, 2793-2802,
766 10.1098/rspb.2014.0882, 2014.

767 Bradley, J. A., Anesio, A. M., Singarayer, J. S., Heath, M. R., and Arndt, S.: SHIMMER (1.0): a
768 novel mathematical model for microbial and biogeochemical dynamics in glacier forefield
769 ecosystems, *Geosci. Model Dev.*, 8, 3441-3470, 10.5194/gmd-8-3441-2015, 2015.

770 Bradley, J. A., Anesio, A., and Arndt, S.: Bridging the divide: a model-data approach to Polar
771 & Alpine Microbiology, *Fems Microbiol Ecol*, 92, 10.1093/femsec/fiw015, 2016.

772 Bratbak, G., and Dundas, I.: Bacterial Dry-Matter Content and Biomass Estimations, *Appl*
773 *Environ Microb*, 48, 755-757, 1984.

774 Brown, S. P., and Jumpponen, A.: Contrasting primary successional trajectories of fungi and
775 bacteria in retreating glacier soils, *Mol Ecol*, 23, 481-497, Doi 10.1111/Mec.12487, 2014.

776 Caporaso, J. G., Kuczynski, J., Stombaugh, J., Bittinger, K., Bushman, F. D., Costello, E. K.,
777 Fierer, N., Pena, A. G., Goodrich, J. K., Gordon, J. I., Huttley, G. A., Kelley, S. T., Knights, D.,
778 Koenig, J. E., Ley, R. E., Lozupone, C. A., McDonald, D., Muegge, B. D., Pirrung, M., Reeder, J.,
779 Sevinsky, J. R., Tumbaugh, P. J., Walters, W. A., Widmann, J., Yatsunenko, T., Zaneveld, J.,
780 and Knight, R.: QIIME allows analysis of high-throughput community sequencing data, *Nat*
781 *Methods*, 7, 335-336, 10.1038/nmeth.f.303, 2010.

782 Cary, S. C., McDonald, I. R., Barrett, J. E., and Cowan, D. A.: On the rocks: the microbiology of
783 Antarctic Dry Valley soils, *Nat Rev Microbiol*, 8, 129-138, 10.1038/nrmicro2281, 2010.

784 Cowan, D. A., Makhalanyane, T. P., Dennis, P. G., and Hopkins, D. W.: Microbial ecology and
785 biogeochemistry of continental Antarctic soils, *Frontiers in microbiology*, 5, Artn 154
786 Doi 10.3389/Fmicb.2014.00154, 2014.

787 Darrah, P. R.: Models of the Rhizosphere .1. Microbial-Population Dynamics around a Root
788 Releasing Soluble and Insoluble Carbon, *Plant Soil*, 133, 187-199, Doi 10.1007/Bf00009191,
789 1991.

790 Dessert, C., Dupre, B., Gaillardet, J., Francois, L. M., and Allegre, C. J.: Basalt weathering laws
791 and the impact of basalt weathering on the global carbon cycle, *Chem Geol*, 202, 257-273,
792 DOI 10.1016/j.chemgeo.2002.10.001, 2003.

793 Duc, L., Noll, M., Meier, B. E., Burgmann, H., and Zeyer, J.: High Diversity of Diazotrophs in
794 the Forefield of a Receding Alpine Glacier, *Microbial Ecol*, 57, 179-190, DOI 10.1007/s00248-
795 008-9408-5, 2009.

796 Dyurgerov, M. B., and Meier, M. F.: Twentieth century climate change: Evidence from small
797 glaciers, *P Natl Acad Sci USA*, 97, 1406-1411, DOI 10.1073/pnas.97.4.1406, 2000.

798 Edgar, R. C., Haas, B. J., Clemente, J. C., Quince, C., and Knight, R.: UCHIME improves
799 sensitivity and speed of chimera detection, *Bioinformatics*, 27, 2194-2200,
800 10.1093/bioinformatics/btr381, 2011.

801 Ensign, K. L., Webb, E. A., and Longstaffe, F. J.: Microenvironmental and seasonal variations
802 in soil water content of the unsaturated zone of a sand dune system at Pinery Provincial
803 Park, Ontario, Canada, *Geoderma*, 136, 788-802, DOI 10.1016/j.geoderma.2006.06.009,
804 2006.

805 Esperschütz, J., Perez-de-Mora, A., Schreiner, K., Welzl, G., Buegger, F., Zeyer, J., Hagedorn,
806 F., Munch, J. C., and Schloter, M.: Microbial food web dynamics along a soil chronosequence
807 of a glacier forefield, *Biogeosciences*, 8, 3283-3294, DOI 10.5194/bg-8-3283-2011, 2011.

808 Filippelli, G. M.: The global phosphorus cycle, *Rev Mineral Geochem*, 48, 391-425, DOI
809 10.2138/rmg.2002.48.10, 2002.

810 Fleming, K. M., Dowdeswell, J. A., and Oerlemans, J.: Modelling the mass balance of
811 northwest Spitsbergen glaciers and responses to climate change, *Annals of Glaciology*, Vol
812 24, 1997, 24, 203-210, 1997.

813 Foereid, B., and Yearsley, J. M.: Modelling the impact of microbial grazers on soluble
814 rhizodeposit turnover, *Plant Soil*, 267, 329-342, DOI 10.1007/s11104-005-0139-9, 2004.

815 Follmi, K. B., Hosein, R., Arn, K., and Steinmann, P.: Weathering and the mobility of
816 phosphorus in the catchments and forefields of the Rhone and Oberaar glaciers, central
817 Switzerland: Implications for the global phosphorus cycle on glacial-interglacial timescales,
818 *Geochim Cosmochim Acta*, 73, 2252-2282, DOI 10.1016/j.gca.2009.01.017, 2009.

819 Fountain, A. G., Nylen, T. H., Tranter, M., and Bagshaw, E.: Temporal variations in physical
820 and chemical features of cryoconite holes on Canada Glacier, McMurdo Dry Valleys,
821 Antarctica, *J Geophys Res-Biogeophys*, 113, Artn G01s92
822 Doi 10.1029/2007jg000430, 2008.

823 Frey, B., Rieder, S. R., Brunner, I., Plotze, M., Koetzsch, S., Lapanje, A., Brandl, H., and Furrer,
824 G.: Weathering-Associated Bacteria from the Damma Glacier Forefield: Physiological
825 Capabilities and Impact on Granite Dissolution, *Appl Environ Microb*, 76, 4788-4796, Doi
826 10.1128/Aem.00657-10, 2010.

827 Frey, B., Buhler, L., Schmutz, S., Zumsteg, A., and Furrer, G.: Molecular characterization of
828 phototrophic microorganisms in the forefield of a receding glacier in the Swiss Alps, *Environ*
829 *Res Lett*, 8, Artn 015033
830 Doi 10.1088/1748-9326/8/1/015033, 2013.

831 Galloway, J. N., Townsend, A. R., Erisman, J. W., Bekunda, M., Cai, Z. C., Freney, J. R.,
832 Martinelli, L. A., Seitzinger, S. P., and Sutton, M. A.: Transformation of the nitrogen cycle:
833 Recent trends, questions, and potential solutions, *Science*, 320, 889-892,
834 10.1126/science.1136674, 2008.

835 Geng, L., Alexander, B., Cole-Dai, J., Steig, E. J., Savarino, J., Sofen, E. D., and Schauer, A. J.:
836 Nitrogen isotopes in ice core nitrate linked to anthropogenic atmospheric acidity change, *P*
837 *Natl Acad Sci USA*, 111, 5808-5812, 10.1073/pnas.1319441111, 2014.

838 Goransson, H., Venterink, H. O., and Baath, E.: Soil bacterial growth and nutrient limitation
839 along a chronosequence from a glacier forefield, *Soil Biol Biochem*, 43, 1333-1340, DOI
840 10.1016/j.soilbio.2011.03.006, 2011.

841 Goulden, M. L., Wofsy, S. C., Harden, J. W., Trumbore, S. E., Crill, P. M., Gower, S. T., Fries, T.,
842 Daube, B. C., Fan, S. M., Sutton, D. J., Bazzaz, A., and Munger, J. W.: Sensitivity of boreal
843 forest carbon balance to soil thaw, *Science*, 279, 214-217, DOI
844 10.1126/science.279.5348.214, 1998.

845 Guelland, K., Esperschütz, J., Bornhauser, D., Bernasconi, S. M., Kretzschmar, R., and
846 Hagedorn, F.: Mineralisation and leaching of C from C-13 labelled plant litter along an initial
847 soil chronosequence of a glacier forefield, *Soil Biol Biochem*, 57, 237-247, DOI
848 10.1016/j.soilbio.2012.07.002, 2013a.

849 Guelland, K., Hagedorn, F., Smittenberg, R. H., Goransson, H., Bernasconi, S. M., Hajdas, I.,
850 and Kretzschmar, R.: Evolution of carbon fluxes during initial soil formation along the
851 forefield of Damma glacier, Switzerland, *Biogeochemistry*, 113, 545-561, DOI
852 10.1007/s10533-012-9785-1, 2013b.

853 Hamilton, T. L., Peters, J. W., Skidmore, M. L., and Boyd, E. S.: Molecular evidence for an
854 active endogenous microbiome beneath glacial ice, *Isme J*, 7, 1402-1412,
855 10.1038/ismej.2013.31, 2013.

856 Hellweger, F. L., and Bucci, V.: A bunch of tiny individuals-Individual-based modeling for
857 microbes, *Ecol Model*, 220, 8-22, DOI 10.1016/j.ecolmodel.2008.09.004, 2009.

858 Hodkinson, I. D., Coulson, S. J., and Webb, N. R.: Community assembly along proglacial
859 chronosequences in the high Arctic: vegetation and soil development in north-west
860 Svalbard, *J Ecol*, 91, 651-663, DOI 10.1046/j.1365-2745.2003.00786.x, 2003.

861 Hodson, A., Anesio, A. M., Ng, F., Watson, R., Quirk, J., Irvine-Fynn, T., Dye, A., Clark, C.,
862 McCloy, P., Kohler, J., and Sattler, B.: A glacier respire: Quantifying the distribution and
863 respiration CO₂ flux of cryoconite across an entire Arctic supraglacial ecosystem, *J Geophys*
864 *Res-Bioge*, 112, Artn G04s36
865 Doi 10.1029/2007jg000452, 2007.

866 Hodson, A., Roberts, T. J., Engvall, A. C., Holmen, K., and Mumford, P.: Glacier ecosystem
867 response to episodic nitrogen enrichment in Svalbard, European High Arctic,
868 *Biogeochemistry*, 98, 171-184, DOI 10.1007/s10533-009-9384-y, 2010.

869 Hodson, A. J., Mumford, P. N., Kohler, J., and Wynn, P. M.: The High Arctic glacial ecosystem:
870 new insights from nutrient budgets, *Biogeochemistry*, 72, 233-256, DOI 10.1007/s10533-
871 004-0362-0, 2005.

872 Ingwersen, J., Poll, C., Streck, T., and Kandeler, E.: Micro-scale modelling of carbon turnover
873 driven by microbial succession at a biogeochemical interface, *Soil Biol Biochem*, 40, 864-878,
874 DOI 10.1016/j.soilbio.2007.10.018, 2008.

875 Insam, H., and Haselwandter, K.: Metabolic Quotient of the Soil Microflora in Relation to
876 Plant Succession, *Oecologia*, 79, 174-178, Doi 10.1007/Bf00388474, 1989.

877 Jakubas, D., Zmudzynska, K., Wojczulanis-Jakubas, K., and Stempniewicz, L.: Faeces
878 deposition and numbers of vertebrate herbivores in the vicinity of planktivorous and
879 piscivorous seabird colonies in Hornsund, Spitsbergen, *Pol Polar Res*, 29, 45-58, 2008.

880 Jessup, C. M., Kassen, R., Forde, S. E., Kerr, B., Buckling, A., Rainey, P. B., and Bohannan, B. J.
881 M.: Big questions, small worlds: microbial model systems in ecology, *Trends Ecol Evol*, 19,
882 189-197, 10.1016/j.tree.2004.01.008, 2004.

883 Johannessen, O. M., Bengtsson, L., Miles, M. W., Kuzmina, S. I., Semenov, V. A., Alekseev, G.
884 V., Nagurnyi, A. P., Zakharov, V. F., Bobylev, L. P., Pettersson, L. H., Hasselmann, K., and
885 Cattle, A. P.: Arctic climate change: observed and modelled temperature and sea-ice
886 variability, *Tellus A*, 56, 328-341, DOI 10.1111/j.1600-0870.2004.00060.x, 2004.

887 Kastovska, K., Elster, J., Stibal, M., and Santruckova, H.: Microbial assemblages in soil
888 microbial succession after glacial retreat in Svalbard (high Arctic), *Microbial Ecol*, 50, 396-
889 407, DOI 10.1007/s00248-005-0246-4, 2005.

890 King, A. J., Meyer, A. F., and Schmidt, S. K.: High levels of microbial biomass and activity in
891 unvegetated tropical and temperate alpine soils, *Soil Biol Biochem*, 40, 2605-2610, DOI
892 10.1016/j.soilbio.2008.06.026, 2008.

893 Kirchman, D.: Measuring Bacterial Biomass Production and Growth Rates from Leucine
894 Incorporation in Natural Aquatic Environments in: *Marine Microbiology*, edited by: Paul, J.
895 H., Academic Press, London, UK, 2001.

896 Kirschke, S., Bousquet, P., Ciais, P., Saunois, M., Canadell, J. G., Dlugokencky, E. J.,
897 Bergamaschi, P., Bergmann, D., Blake, D. R., Bruhwiler, L., Cameron-Smith, P., Castaldi, S.,
898 Chevallier, F., Feng, L., Fraser, A., Heimann, M., Hodson, E. L., Houweling, S., Josse, B.,
899 Fraser, P. J., Krummel, P. B., Lamarque, J. F., Langenfelds, R. L., Le Quere, C., Naik, V.,
900 O'Doherty, S., Palmer, P. I., Pison, I., Plummer, D., Poulter, B., Prinn, R. G., Rigby, M.,
901 Ringeval, B., Santini, M., Schmidt, M., Shindell, D. T., Simpson, I. J., Spahni, R., Steele, L. P.,
902 Strobe, S. A., Sudo, K., Szopa, S., van der Werf, G. R., Voulgarakis, A., van Weele, M., Weiss,

903 R. F., Williams, J. E., and Zeng, G.: Three decades of global methane sources and sinks, *Nat*
904 *Geosci*, 6, 813-823, Doi 10.1038/Ngeo1955, 2013.

905 Knapp, E. B., Elliott, L. F., and Campbell, G. S.: Carbon, Nitrogen and Microbial Biomass
906 Interrelationships during the Decomposition of Wheat Straw - a Mechanistic Simulation-
907 Model, *Soil Biol Biochem*, 15, 455-461, Doi 10.1016/0038-0717(83)90011-1, 1983.

908 Kuhnel, R., Roberts, T. J., Bjorkman, M. P., Isaksson, E., Aas, W., Holmen, K., and Strom, J.:
909 20-Year Climatology of NO₃⁻ and NH₄⁺ Wet Deposition at Ny-Alesund, Svalbard, *Adv*
910 *Meteorol*, Artn 406508
911 Doi 10.1155/2011/406508, 2011.

912 Kuhnel, R., Bjorkman, M. P., Vega, C. P., Hodson, A., Isaksson, E., and Strom, J.: Reactive
913 nitrogen and sulphate wet deposition at Zeppelin Station, Ny-Alesund, Svalbard, *Polar Res*,
914 32, Unsp 19136
915 Doi 10.3402/Polar.V32i0.19136, 2013.

916 Larsen, P., Hamada, Y., and Gilbert, J.: Modeling microbial communities: Current,
917 developing, and future technologies for predicting microbial community interaction, *J*
918 *Biotechnol*, 160, 17-24, 10.1016/j.jbiotec.2012.03.009, 2012.

919 Lazzaro, A., Brankatschk, R., and Zeyer, J.: Seasonal dynamics of nutrients and bacterial
920 communities in unvegetated alpine glacier forefields, *Appl Soil Ecol*, 53, 10-22, DOI
921 10.1016/j.apsoil.2011.10.013, 2012.

922 Lazzaro, A., Hilfiker, D., and Zeyer, J.: Structures of Microbial Communities in Alpine Soils:
923 Seasonal and Elevational Effects, *Frontiers in microbiology*, 6, ARTN 1330
924 10.3389/fmicb.2015.01330, 2015.

925 Lee, S.: A theory for polar amplification from a general circulation perspective, *Asia-Pac J*
926 *Atmos Sci*, 50, 31-43, DOI 10.1007/s13143-014-0024-7, 2014.

927 Luoto, T. P., Oksman, M., and Ojala, A. E. K.: Climate change and bird impact as drivers of
928 High Arctic pond deterioration, *Polar Biol*, 38, 357-368, 10.1007/s00300-014-1592-9, 2015.

929 Lutz, S., Anesio, A. M., Villar, S. E. J., and Benning, L. G.: Variations of algal communities
930 cause darkening of a Greenland glacier, *Fems Microbiol Ecol*, 89, 402-414, 10.1111/1574-
931 6941.12351, 2014.

932 Lutz, S., Anesio, A. M., Edwards, A., and Benning, L. G.: Microbial diversity on Icelandic
933 glaciers and ice caps, *Frontiers in microbiology*, 6, ARTN 307
934 10.3389/fmicb.2015.00307, 2015.

935 Manzoni, S., Porporato, A., D'Odorico, P., Laio, F., and Rodriguez-Iturbe, I.: Soil nutrient
936 cycles as a nonlinear dynamical system, *Nonlinear Proc Geoph*, 11, 589-598, 2004.

937 Manzoni, S., and Porporato, A.: A theoretical analysis of nonlinearities and feedbacks in soil
938 carbon and nitrogen cycles, *Soil Biol Biochem*, 39, 1542-1556, 10.1016/j.soilbio.2007.01.006,
939 2007.

940 Mapelli, F., Marasco, R., Rizzi, A., Baldi, F., Ventura, S., Daffonchio, D., and Borin, S.: Bacterial
941 Communities Involved in Soil Formation and Plant Establishment Triggered by Pyrite
942 Bioweathering on Arctic Moraines, *Microbial Ecol*, 61, 438-447, 10.1007/s00248-010-9758-
943 7, 2011.

944 McDonald, D., Price, M. N., Goodrich, J., Nawrocki, E. P., DeSantis, T. Z., Probst, A.,
945 Andersen, G. L., Knight, R., and Hugenholtz, P.: An improved Greengenes taxonomy with
946 explicit ranks for ecological and evolutionary analyses of bacteria and archaea, *Isme J*, 6,
947 610-618, 10.1038/ismej.2011.139, 2012.

948 Michelutti, N., Keatley, B. E., Brimble, S., Blais, J. M., Liu, H. J., Douglas, M. S. V., Mallory, M.
949 L., Macdonald, R. W., and Smol, J. P.: Seabird-driven shifts in Arctic pond ecosystems, *P Roy*
950 *Soc B-Biol Sci*, 276, 591-596, DOI 10.1098/rspb.2008.1103, 2009.

951 Michelutti, N., Mallory, M. L., Blais, J. M., Douglas, M. S. V., and Smol, J. P.: Chironomid
952 assemblages from seabird-affected High Arctic ponds, *Polar Biol*, 34, 799-812,
953 DOI 10.1007/s00300-010-0934-5, 2011.

954 Mindl, B., Anesio, A. M., Meirer, K., Hodson, A. J., Laybourn-Parry, J., Sommaruga, R., and
955 Sattler, B.: Factors influencing bacterial dynamics along a transect from supraglacial runoff
956 to proglacial lakes of a high Arctic glacier (vol 7, pg 307, 2007), *Fems Microbiol Ecol*, 59,
957 762-762, DOI 10.1111/j.1574-6941.2007.00295.x, 2007.

958 Moe, B., Stempniewicz, L., Jakubas, D., Angelier, F., Chastel, O., Dinessen, F., Gabrielsen, G.
959 W., Hanssen, F., Karnovsky, N. J., Ronning, B., Welcker, J., Wojczulanis-Jakubas, K., and Bech,
960 C.: Climate change and phenological responses of two seabird species breeding in the high-
961 Arctic, *Mar Ecol Prog Ser*, 393, 235-246, DOI 10.3354/meps08222, 2009.

962 Moreau, M., Mercier, D., Laffly, D., and Roussel, E.: Impacts of recent paraglacial dynamics
963 on plant colonization: A case study on Midtre Lovenbreen foreland, Spitsbergen (79 degrees
964 N), *Geomorphology*, 95, 48-60, DOI 10.1016/j.geomorph.2006.07.031, 2008.

965 Moritz, R. E., Bitz, C. M., and Steig, E. J.: Dynamics of recent climate change in the Arctic,
966 *Science*, 297, 1497-1502, DOI 10.1126/science.1076522, 2002.

967 Oechel, W. C., Hastings, S. J., Vourlitis, G., Jenkins, M., Riechers, G., and Grulke, N.: Recent
968 Change of Arctic Tundra Ecosystems from a Net Carbon-Dioxide Sink to a Source, *Nature*,
969 361, 520-523, DOI 10.1038/361520a0, 1993.

970 Oechel, W. C., Vourlitis, G. L., Hastings, S. J., Zulueta, R. C., Hinzman, L., and Kane, D.:
971 Acclimation of ecosystem CO₂ exchange in the Alaskan Arctic in response to decadal climate
972 warming, *Nature*, 406, 978-981, DOI 10.1038/35023137, 2000.

973 Paul, F., Frey, H., and Le Bris, R.: A new glacier inventory for the European Alps from Landsat
974 TM scenes of 2003: challenges and results, *Ann Glaciol*, 52, 144-152, 2011.

975 Prietzel, J., Dumig, A., Wu, Y. H., Zhou, J., and Klysubun, W.: Synchrotron-based P K-edge
976 XANES spectroscopy reveals rapid changes of phosphorus speciation in the topsoil of two
977 glacier foreland chronosequences, *Geochim Cosmochim Acta*, 108, 154-171, DOI
978 10.1016/j.gca.2013.01.029, 2013.

979 Schipper, L. A., Hobbs, J. K., Rutledge, S., and Arcus, V. L.: Thermodynamic theory explains
980 the temperature optima of soil microbial processes and high Q₁₀ values at low
981 temperatures, *Global Change Biol*, 20, 3578-3586, DOI 10.1111/Gcb.12596, 2014.

982 Schloss, P. D., Westcott, S. L., Ryabin, T., Hall, J. R., Hartmann, M., Hollister, E. B., Lesniewski,
983 R. A., Oakley, B. B., Parks, D. H., Robinson, C. J., Sahl, J. W., Stres, B., Thallinger, G. G., Van
984 Horn, D. J., and Weber, C. F.: Introducing mothur: Open-Source, Platform-Independent,
985 Community-Supported Software for Describing and Comparing Microbial Communities, *Appl*
986 *Environ Microb*, 75, 7537-7541, DOI 10.1128/Aem.01541-09, 2009.

987 Schmidt, S. K., Reed, S. C., Nemergut, D. R., Grandy, A. S., Cleveland, C. C., Weintraub, M. N.,
988 Hill, A. W., Costello, E. K., Meyer, A. F., Neff, J. C., and Martin, A. M.: The earliest stages of
989 ecosystem succession in high-elevation (5000 metres above sea level), recently deglaciated
990 soils, *P Roy Soc B-Biol Sci*, 275, 2793-2802, DOI 10.1098/rspb.2008.0808, 2008.

991 Schostag, M., Stibal, M., Jacobsen, C. S., Baelum, J., Tas, N., Elberling, B., Jansson, J. K.,
992 Semenchuk, P., and Prieme, A.: Distinct summer and winter bacterial communities in the
993 active layer of Svalbard permafrost revealed by DNA- and RNA-based analyses, *Frontiers in*
994 *microbiology*, 6, ARTN 399

995 10.3389/fmicb.2015.00399, 2015.

996 Schulz, S., Brankatschk, R., Dumig, A., Kogel-Knabner, I., Schloter, M., and Zeyer, J.: The role
997 of microorganisms at different stages of ecosystem development for soil formation,
998 *Biogeosciences*, 10, 3983-3996, DOI 10.5194/bg-10-3983-2013, 2013.

999 Schutte, U. M. E., Abdo, Z., Bent, S. J., Williams, C. J., Schneider, G. M., Solheim, B., and
1000 Forney, L. J.: Bacterial succession in a glacier foreland of the High Arctic, *Isme J*, 3, 1258-
1001 1268, DOI 10.1038/ismej.2009.71, 2009.

1002 Scott, E. M., Rattray, E. A. S., Prosser, J. I., Killham, K., Glover, L. A., Lynch, J. M., and Bazin,
1003 M. J.: A Mathematical-Model for Dispersal of Bacterial Inoculants Colonizing the Wheat
1004 Rhizosphere, *Soil Biol Biochem*, 27, 1307-1318, Doi 10.1016/0038-0717(95)00050-O, 1995.

1005 Serreze, M. C., Walsh, J. E., Chapin, F. S., Osterkamp, T., Dyurgerov, M., Romanovsky, V.,
1006 Oechel, W. C., Morison, J., Zhang, T., and Barry, R. G.: Observational evidence of recent
1007 change in the northern high-latitude environment, *Climatic Change*, 46, 159-207, Doi
1008 10.1023/A:1005504031923, 2000.

1009 Servedio, M. R., Brandvain, Y., Dhole, S., Fitzpatrick, C. L., Goldberg, E. E., Stern, C. A., Van
1010 Cleve, J., and Yeh, D. J.: Not just a theory--the utility of mathematical models in evolutionary
1011 biology, *Plos Biol*, 12, e1002017, 10.1371/journal.pbio.1002017, 2014.

1012 Simon, M., and Azam, F.: Protein-Content and Protein-Synthesis Rates of Planktonic Marine-
1013 Bacteria, *Mar Ecol Prog Ser*, 51, 201-213, DOI 10.3354/meps051201, 1989.

1014 Smittenberg, R. H., Gierga, M., Goransson, H., Christl, I., Farinotti, D., and Bernasconi, S. M.:
1015 Climate-sensitive ecosystem carbon dynamics along the soil chronosequence of the Damma
1016 glacier forefield, Switzerland, *Global Change Biol*, 18, 1941-1955, DOI 10.1111/j.1365-
1017 2486.2012.02654.x, 2012.

1018 Soetaert, K., and Herman, P.: *A Practical Guide to Ecological Modelling: Using R as a*
1019 *Simulation Platform*, Springer, UK, 2009.

1020 Staines, K. E. H., Carrivick, J. L., Tweed, F. S., Evans, A. J., Russell, A. J., Jóhannesson, T., and
1021 Roberts, M.: A multi-dimensional analysis of pro-glacial landscape change at Sólheimajökull,
1022 southern Iceland, *Earth Surface Processes and Landforms*, 40, 809-822, 10.1002/esp.3662,
1023 2014.

1024 Stapleton, L. M., Crout, N. M. J., Sawstrom, C., Marshall, W. A., Poulton, P. R., Tye, A. M.,
1025 and Laybourn-Parry, J.: Microbial carbon dynamics in nitrogen amended Arctic tundra soil:
1026 Measurement and model testing, *Soil Biol Biochem*, 37, 2088-2098, DOI
1027 10.1016/j.soilbio.2005.03.016, 2005.

1028 Stibal, M., Tranter, M., Benning, L. G., and Rehak, J.: Microbial primary production on an
1029 Arctic glacier is insignificant in comparison with allochthonous organic carbon input, *Environ*
1030 *Microbiol*, 10, 2172-2178, 10.1111/j.1462-2920.2008.01620.x, 2008.

1031 Strauss, S. L., Garcia-Pichel, F., and Day, T. A.: Soil microbial carbon and nitrogen
1032 transformations at a glacial foreland on Anvers Island, Antarctic Peninsula, *Polar Biol*, 35,
1033 1459-1471, DOI 10.1007/s00300-012-1184-5, 2012.

1034 Telling, J., Anesio, A. M., Tranter, M., Irvine-Fynn, T., Hodson, A., Butler, C., and Wadham, J.:
1035 Nitrogen fixation on Arctic glaciers, Svalbard, *J Geophys Res-Bioge*, 116, Artn G03039
1036 Doi 10.1029/2010jg001632, 2011.

1037 Telling, J., Stibal, M., Anesio, A. M., Tranter, M., Nias, I., Cook, J., Bellas, C., Lis, G., Wadham,
1038 J. L., Sole, A., Nienow, P., and Hodson, A.: Microbial nitrogen cycling on the Greenland Ice
1039 Sheet, *Biogeosciences*, 9, 2431-2442, 10.5194/bg-9-2431-2012, 2012.

1040 Toal, M. E., Yeomans, C., Killham, K., and Meharg, A. A.: A review of rhizosphere carbon flow
1041 modelling, *Plant Soil*, 222, 263-281, Doi 10.1023/A:1004736021965, 2000.

1042 Tscherko, D., Rustemeier, J., Richter, A., Wanek, W., and Kandeler, E.: Functional diversity of
1043 the soil microflora in primary succession across two glacier forelands in the Central Alps, Eur
1044 J Soil Sci, 54, 685-696, DOI 10.1046/j.1365-2389.2003.00570.x, 2003.

1045 Vandewerf, H., and Verstraete, W.: Estimation of Active Soil Microbial Biomass by
1046 Mathematical-Analysis of Respiration Curves - Development and Verification of the Model,
1047 Soil Biol Biochem, 19, 253-260, Doi 10.1016/0038-0717(87)90006-X, 1987.

1048 Wang, Y. P., Chen, B. C., Wieder, W. R., Leite, M., Medlyn, B. E., Rasmussen, M., Smith, M. J.,
1049 Agosto, F. B., Hoffman, F., and Luo, Y. Q.: Oscillatory behavior of two nonlinear microbial
1050 models of soil carbon decomposition, Biogeosciences, 11, 1817-1831, 10.5194/bg-11-1817-
1051 2014, 2014.

1052 Yde, J. C., Finster, K. W., Raiswell, R., Steffensen, J. P., Heinemeier, J., Olsen, J.,
1053 Gunnlaugsson, H. P., and Nielsen, O. B.: Basal ice microbiology at the margin of the
1054 Greenland ice sheet, Ann Glaciol, 51, 71-79, 2010.

1055 Yoshitake, S., Uchida, M., Koizumi, H., Kanda, H., and Nakatsubo, T.: Production of biological
1056 soil crusts in the early stage of primary succession on a High Arctic glacier foreland, New
1057 Phytol, 186, 451-460, DOI 10.1111/j.1469-8137.2010.03180.x, 2010.

1058 Zdanowski, M. K., Zmuda-Baranowska, M. J., Borsuk, P., Swiatecki, A., Gorniak, D., Wolicka,
1059 D., Jankowska, K. M., and Grzesiak, J.: Culturable bacteria community development in
1060 postglacial soils of Ecology Glacier, King George Island, Antarctica, Polar Biol, 36, 511-527,
1061 DOI 10.1007/s00300-012-1278-0, 2013.

1062 Zelenev, V. V., van Bruggen, A. H. C., and Semenov, A. M.: "BACWAVE," a spatial-temporal
1063 model for traveling waves of bacterial populations in response to a moving carbon source in
1064 soil, Microbial Ecol, 40, 260-272, 2000.

1065 Zhang, X. Y., Wang, W., Chen, W. L., Zhang, N. L., and Zeng, H.: Comparison of Seasonal Soil
1066 Microbial Process in Snow-Covered Temperate Ecosystems of Northern China, Plos One, 9,
1067 ARTN e92985
1068 10.1371/journal.pone.0092985, 2014.

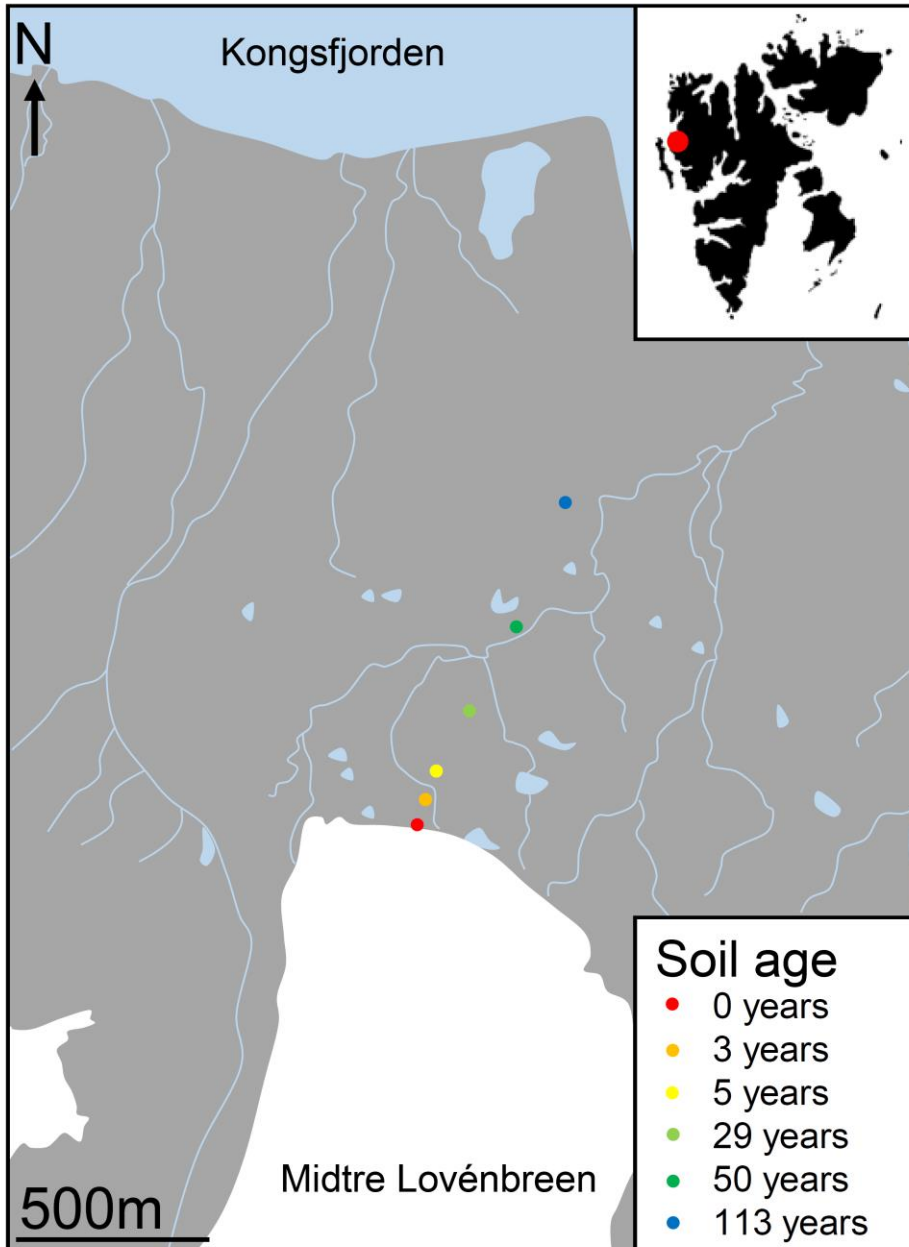
1069 Ziolk, M., and Melke, J.: The impact of seabirds on the content of various forms of
1070 phosphorus in organic soils of the Bellsund coast, western Spitsbergen, Polar Res, 33, ARTN
1071 19986
1072 10.3402/polar.v33.19986, 2014.

1073 Zumsteg, A., Bernasconi, S. M., Zeyer, J., and Frey, B.: Microbial community and activity
1074 shifts after soil transplantation in a glacier forefield, Appl Geochem, 26, S326-S329, DOI
1075 10.1016/j.apgeochem.2011.03.078, 2011.

1076 Zumsteg, A., Luster, J., Goransson, H., Smittenberg, R. H., Brunner, I., Bernasconi, S. M.,
1077 Zeyer, J., and Frey, B.: Bacterial, Archaeal and Fungal Succession in the Forefield of a
1078 Receding Glacier, Microbial Ecol, 63, 552-564, DOI 10.1007/s00248-011-9991-8, 2012.

1079 Zumsteg, A., Schmutz, S., and Frey, B.: Identification of biomass utilizing bacteria in a
1080 carbon-depleted glacier forefield soil by the use of ¹³C DNA stable isotope probing, Env
1081 Microbiol Rep, 5, 424-437, Doi 10.1111/1758-2229.12027, 2013.

1082
1083
1084
1085
1086
1087
1088
1089



1090

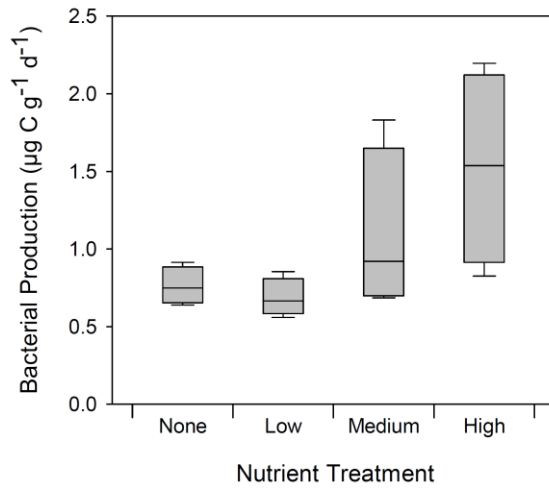
1091

Figure 1. Midtre Lovénbreen glacier and forefield in Svalbard, the location of sampling sites and approximate age of soil.

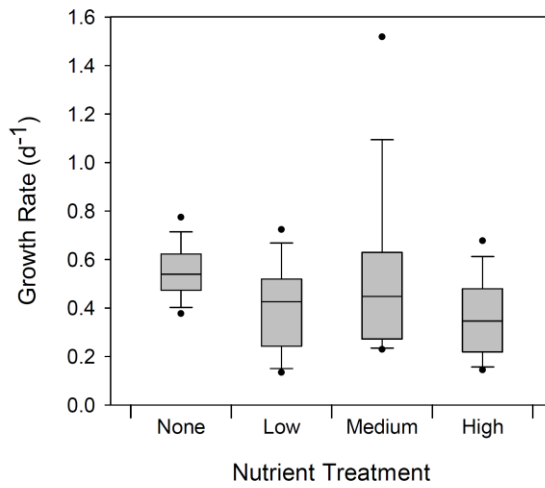
1092

1093

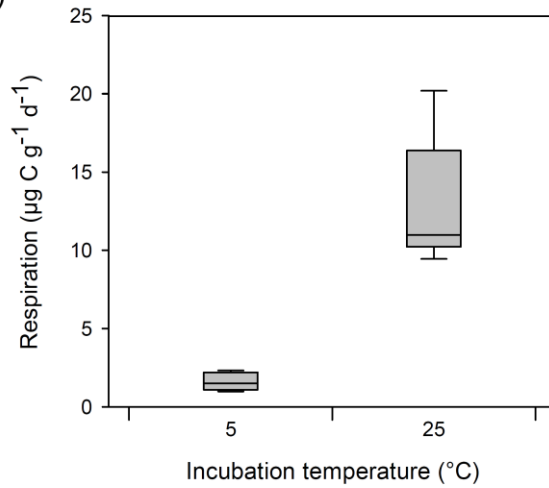
(a)



(b)



(c)



1094

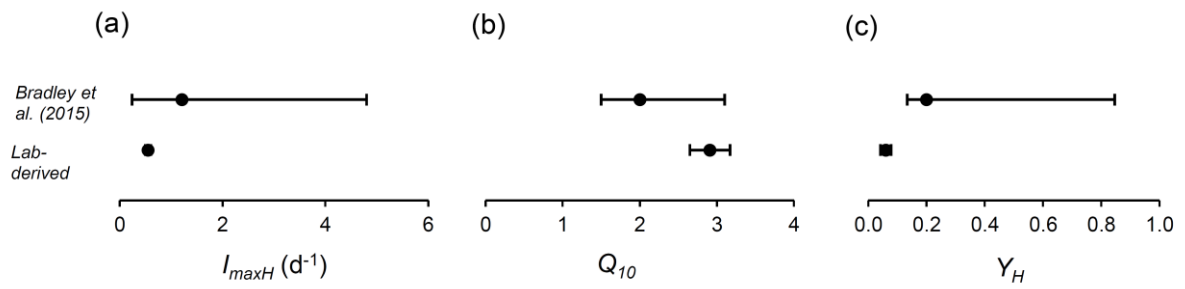
1095 Figure 2. Measurements of (a) bacterial carbon production and (b) growth rate, derived from ^3H -

1096 leucine assays at different nutrient conditions, and (c) bacterial respiration at 5°C and 25°C.

1097

1098

1099

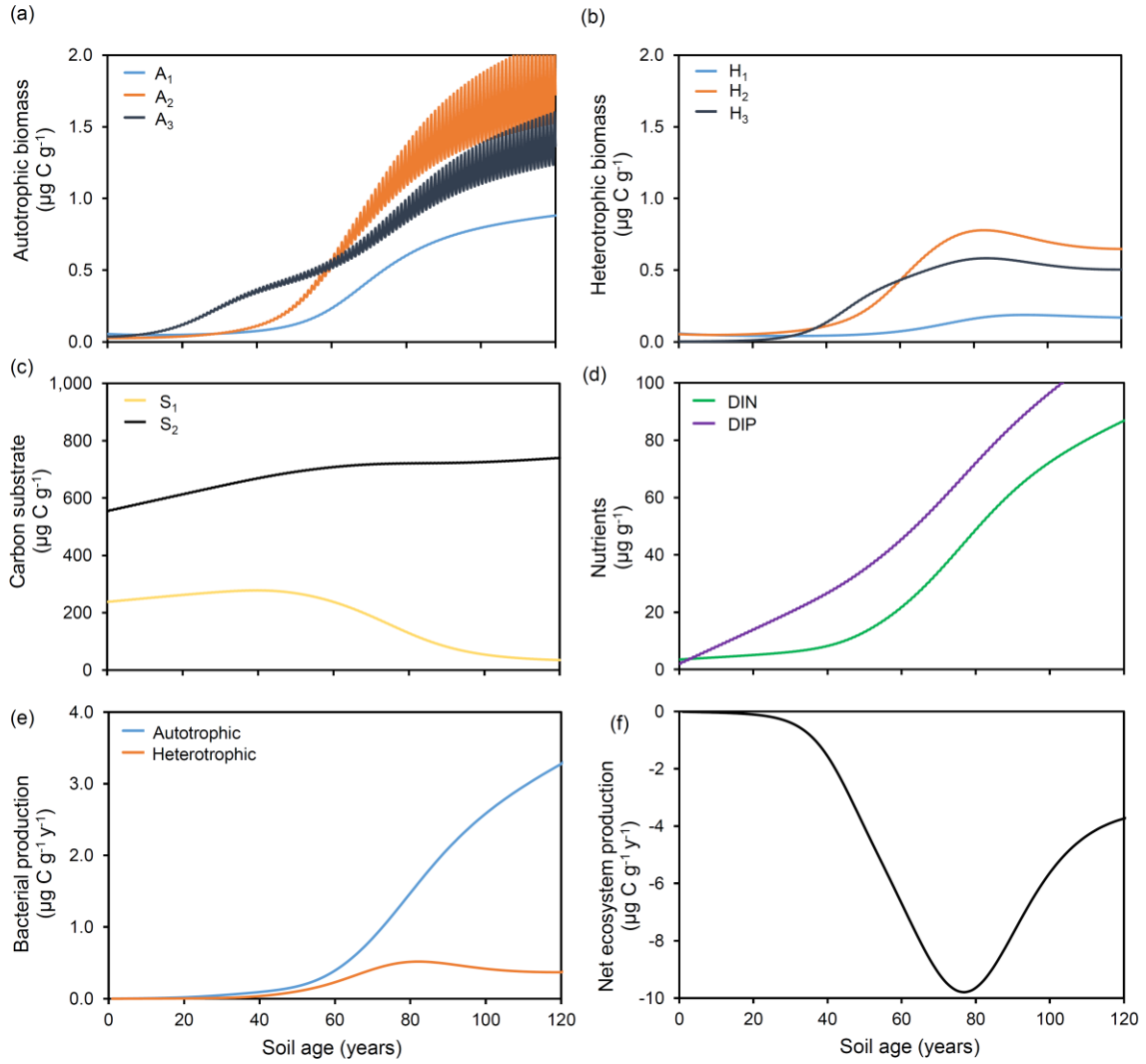


1100

1101

1102

1103 Figure 3. A comparison of previously established ranges for parameters (Bradley et al., 2015) with
1104 laboratory-derived values for (a) maximum growth rate (I_{max}), (b) temperature response (Q_{10}), (c) BGE
1105 (Y).
1106



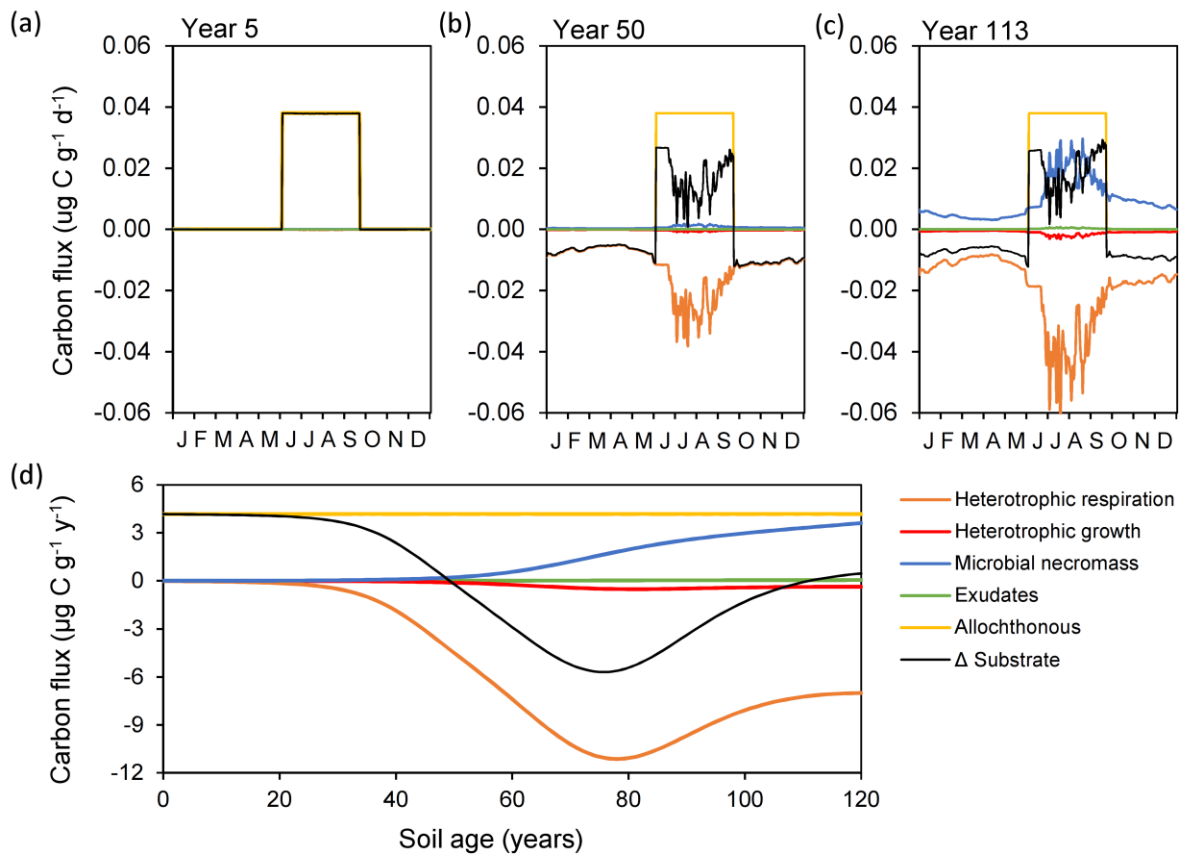
1107

1108 Figure 4. Modelled (a) autotrophic biomass, (b) heterotrophic biomass, (c) carbon substrate, (d)

1109 nutrients, (e) bacterial production and (f) net ecosystem production, with laboratory-derived parameter

1110 values.

1111



1112

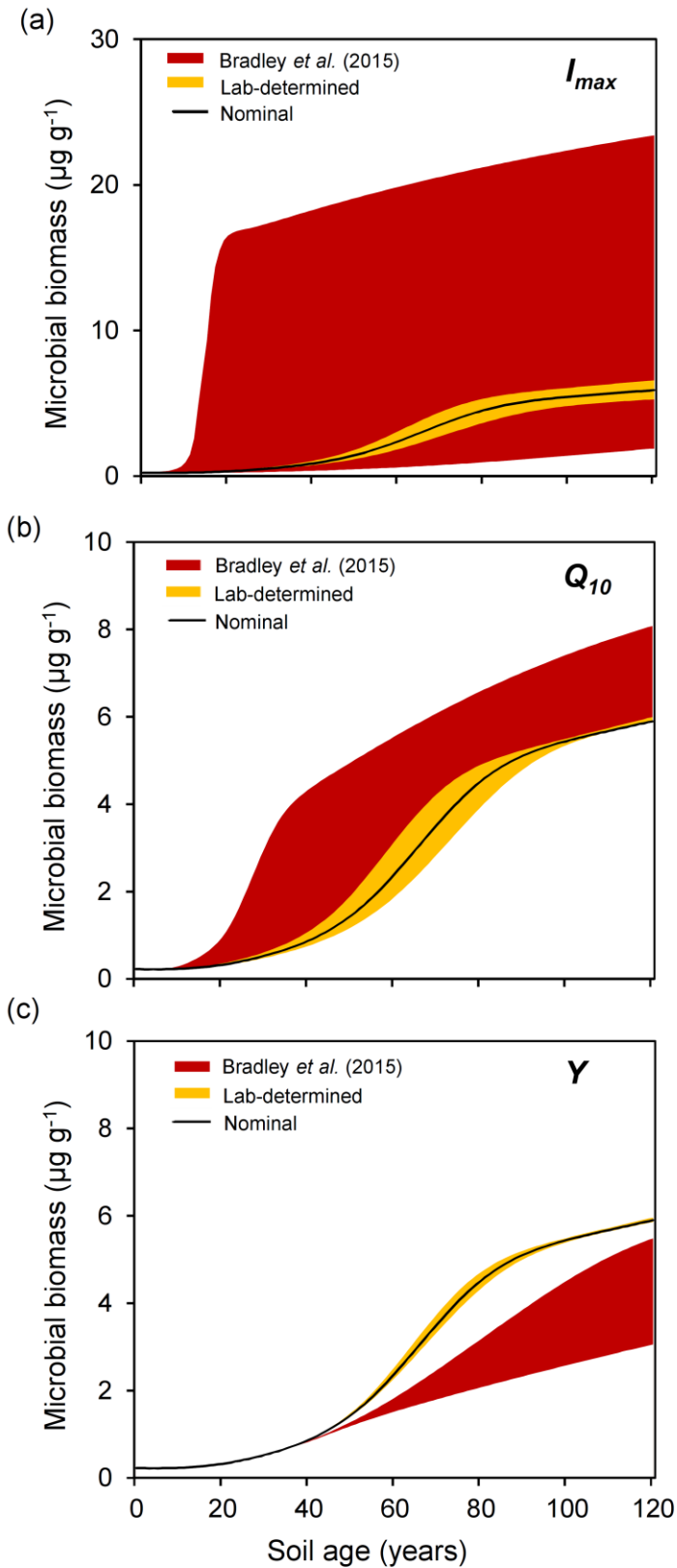
1113 Figure 5. Illustration of daily carbon fluxes for (a) 5, (b) 50 and (c) 113 year old soil, and (d) annual

1114 carbon flux over 120 years. Microbial necromass (blue), exudates (green) and allochthonous sources

1115 (yellow) contribute to the substrate pool (black), and heterotrophic growth (red) and respiration

1116 (orange) deplete it.

1117



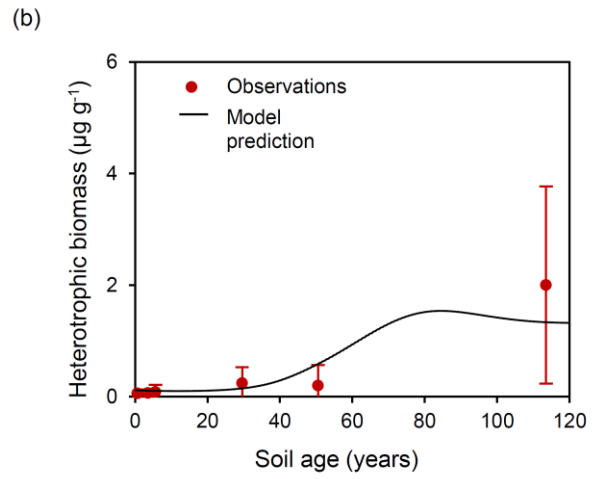
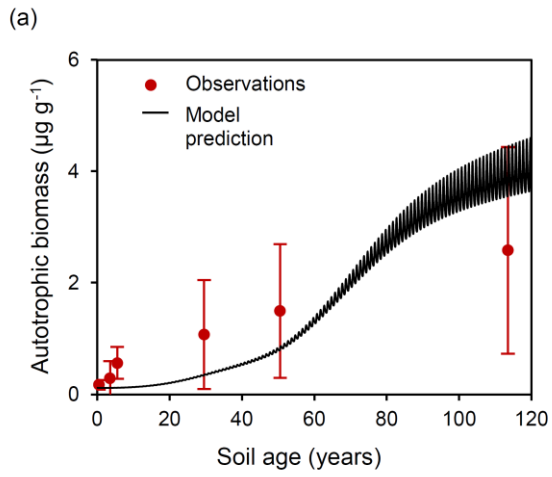
1118

1119 Figure 6. A comparison of predicted microbial biomass with laboratory-derived parameter values

1120 (yellow) and previously established parameter values (Bradley *et al.*, 2015) (red) for variation in the

1121 following parameters: (a) maximum growth rate (I_{max}), (b) temperature response (Q_{10}), (c) BGE (Y).

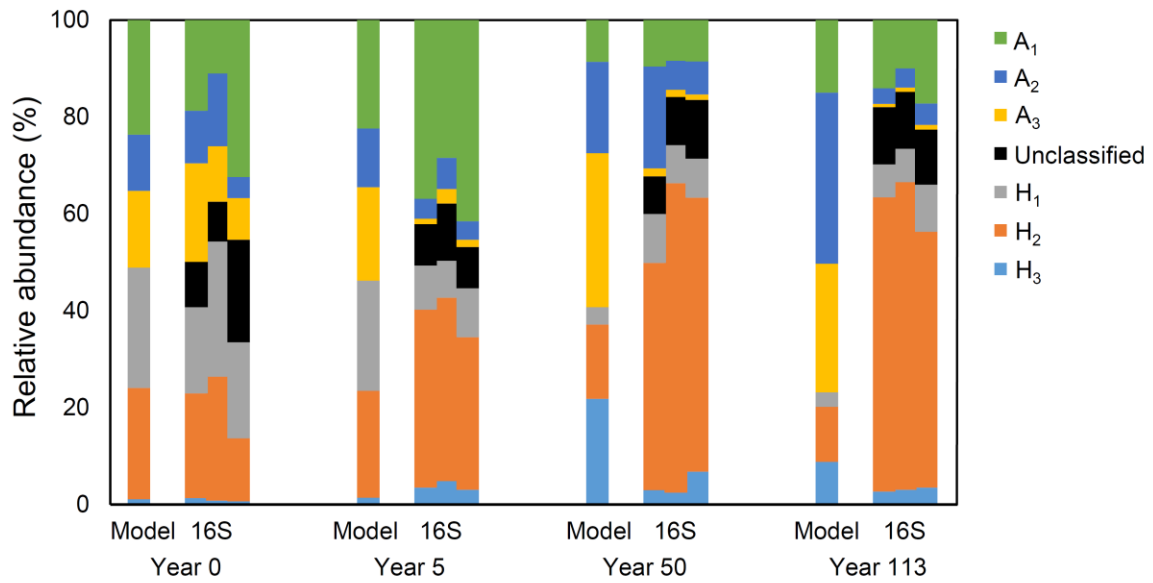
1122



1123

1124 Figure 7. Model predictions of (a) autotrophic and (b) heterotrophic biomass (black line), compared to
1125 observational data (red) derived from microscopy.

1126



1127

1128

Figure 8. A comparison of microbial diversity from model output and genomic analyses at 0 year old,

1129

5 year old, 50 year old and 113 year old soil.

1130

1131

1132

1133

1134 Table 1. State variables and initial values.

State Variable	Units	Description	Initial value (year 0) ($\mu\text{g g}^{-1}$)
A ₁	$\mu\text{g C g}^{-1}$	Subglacial chemolithoautotrophs	<i>0.0547</i>
A ₂	$\mu\text{g C g}^{-1}$	Soil autotrophs	<i>0.0266</i>
A ₃	$\mu\text{g C g}^{-1}$	Nitrogen fixing soil autotrophs	<i>0.0355</i>
H ₁	$\mu\text{g C g}^{-1}$	Subglacial heterotrophs	<i>0.0576</i>
H ₂	$\mu\text{g C g}^{-1}$	Soil heterotrophs	<i>0.0530</i>
H ₃	$\mu\text{g C g}^{-1}$	Nitrogen fixing soil heterotrophs	<i>0.0025</i>
S ₁	$\mu\text{g C g}^{-1}$	Labile organic carbon	<i>291.895</i>
S ₂	$\mu\text{g C g}^{-1}$	Refractory organic carbon	<i>681.089</i>
DIN	$\mu\text{g N g}^{-1}$	Dissolved inorganic nitrogen (DIN)	<i>3.530</i>
DIP	$\mu\text{g P g}^{-1}$	Dissolved inorganic phosphorus (DIP)	<i>2.078</i>
ON ₁	$\mu\text{g N g}^{-1}$	Labile organic nitrogen	<i>41.157</i>
ON ₂	$\mu\text{g N g}^{-1}$	Refractory organic nitrogen	<i>96.034</i>
OP ₁	$\mu\text{g P g}^{-1}$	Labile organic phosphorus	<i>24.227</i>
OP ₂	$\mu\text{g P g}^{-1}$	Refractory organic phosphorus	<i>56.530</i>

1135

1136

1137

1138

1139 Table 2. Microbial biomass in the forefield of Midtre Lovénbreen (brackets show 1 standard deviation)
 1140

Soil Age (years)	Autotrophic biomass ($\mu\text{g C g}^{-1}$)	Heterotrophic biomass ($\mu\text{g C g}^{-1}$)	Total Organic Carbon ($\mu\text{g C g}^{-1}$)
0	0.171 (0.042)	0.059 (0.034)	792.984 (127.206)
3	0.287 (0.155)	0.064 (0.029)	
5	0.561 (0.143)	0.083 (0.065)	
29	1.072 (0.487)	0.244 (0.142)	
50	1.497 (0.601)	0.197 (0.184)	
113	2.581 (0.927)	2.000 (0.885)	

1141
 1142
 1143
 1144
 1145
 1146

1147 Table 3. Model output.

Soil Age (years)	Autotrophic biomass ($\mu\text{g C g}^{-1}$)	Heterotrophic biomass ($\mu\text{g C g}^{-1}$)	Autotrophic production ($\mu\text{g C g}^{-1} \text{y}^{-1}$)	Heterotrophic production ($\mu\text{g C g}^{-1} \text{y}^{-1}$)	Net ecosystem production ($\mu\text{g C g}^{-1} \text{y}^{-1}$)	DIN assimilation ($\mu\text{g N g}^{-1} \text{y}^{-1}$)	N_2 fixation ($\mu\text{g N g}^{-1} \text{y}^{-1}$)
0	0.117	0.111	0.002	0.001	- 0.011	2.0×10^{-4}	2.0×10^{-4}
3	0.117	0.105	0.003	0.001	- 0.020	3.0×10^{-4}	3.0×10^{-4}
5	0.119	0.102	0.004	0.001	- 0.025	4.0×10^{-4}	4.0×10^{-4}
29	0.359	0.147	0.050	0.012	- 0.391	0.002	0.006
50	0.860	0.591	0.187	0.113	- 4.311	0.022	0.021
113	4.414	1.331	3.093	0.376	- 4.031	0.458	0.031

1148
 1149
 1150
 1151
 1152
 1153
 1154